

All-Russia Scientific Research Institute of Experimental Physics

607200, Arzamas-16, Nizhni Novgorod region Russian Federation

Fax: 8313054565 Telex: 151109 ARSA

**STUDY OF IMPLoding LINER - ELECTRODE WALL INTERACTION**

The authors:

Chernyshev V.K., Zharinov Ye. I., Kudolkin I.D., Ruzin V.N.,  
Ionov A. I., Grinevich B. Ye., Bidylo N.P., Zimakov S.D.,  
Sokolova O.V., Yerichev V.N., Yegorychev B.T., Shaidulin V.Sh.,  
Mokhov V.N., Garanin S.F.

**A R E P O R T**

under the contract N F61708 - 94 - C - 0014, made between  
"Phillips laboratory " (USA) and Russian Federal Nuclear  
Center VNIIEF (Russia)

Technical representative of VNIIEF  
Professor

 Vladimir K. Chernyshev

Reproduced From  
Best Available Copy

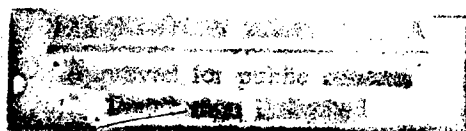
28. 12. 94

DTIC QUALITY INSPECTED 4

19990204 015

- 1994 -

AQ F 99-05- 0845



**REPORT DOCUMENTATION PAGE**

Form Approved OMB No. 0704-0188

Public reporting burden for this collection of information is estimated to average 1 hour per response, including the time for reviewing instructions, searching existing data sources, gathering and maintaining the data needed, and completing and reviewing the collection of information. Send comments regarding this burden estimate or any other aspect of this collection of information, including suggestions for reducing this burden to Washington Headquarters Services, Directorate for Information Operations and Reports, 1215 Jefferson Davis Highway, Suite 1204, Arlington, VA 22202-4302, and to the Office of Management and Budget, Paperwork Reduction Project (0704-0188), Washington, DC 20503.

1. AGENCY USE ONLY (Leave blank)		2. REPORT DATE  December 1994	3. REPORT TYPE AND DATES COVERED  Final Report	
4. TITLE AND SUBTITLE  Study of Emploding Liner - Electrode Wall Interaction			5. FUNDING NUMBERS  F6170894	
6. AUTHOR(S)  Dr Vladimir Chernyshev				
7. PERFORMING ORGANIZATION NAME(S) AND ADDRESS(ES)  All-Russia Scientific Research Institute of Experimental Physics Sarov Arzamas-16 607200 Russia			8. PERFORMING ORGANIZATION REPORT NUMBER  N/A	
9. SPONSORING/MONITORING AGENCY NAME(S) AND ADDRESS(ES)  EOARD PSC 802 BOX 14 FPO 09499-0200			10. SPONSORING/MONITORING AGENCY REPORT NUMBER  SPC 94-4057	
11. SUPPLEMENTARY NOTES				
12a. DISTRIBUTION/AVAILABILITY STATEMENT  Approved for public release; distribution is unlimited.			12b. DISTRIBUTION CODE  A	
13. ABSTRACT (Maximum 200 words)  This report results from a contract tasking All-Russia Scientific Research Institute of Experimental Physics as follows: Perform a series of four convergence liner experiments to study instabilities due to walls-liner interactions in explosive magnetic generators. The Phillips Lab and VNIIEF will jointly define all experimental set-ups and diagnostics for the tests.				
14. SUBJECT TERMS  EOARD			15. NUMBER OF PAGES  48	
			16. PRICE CODE N/A	
17. SECURITY CLASSIFICATION OF REPORT  UNCLASSIFIED	18. SECURITY CLASSIFICATION OF THIS PAGE  UNCLASSIFIED	19. SECURITY CLASSIFICATION OF ABSTRACT  UNCLASSIFIED	20. LIMITATION OF ABSTRACT  UL	

NSN 7540-01-280-5500

Standard Form 298 (Rev. 2-89)  
Prescribed by ANSI Std. Z39-18  
298-102

We conducted experiments to study instabilities, developed, when a liner, converged under magnetic field, interacted with electrode walls.

A liner was compressed by a current pulse with an amplitude of  $\sim 5$  MA and effective time of  $\sim 17$   $\mu$ sec.

Initial conditions were: a liner with a radius of  $R_0 = 30$  mm, a relative length of  $L/R_0 = 1$ , aspect ratio of  $R_0/\Delta = 30$ ; a liner and electrodes were made of aluminum.

In each experiment two liners were used. One was located between straight walls ( $\alpha = 0^\circ$ ), the walls of another were slightly inclined ( $\alpha = 3^\circ$ ).

In the first experiment liners were connected with electrodes in a sliding fit manner at the depth of 0,5 mm.

At the radius of 0,5  $R_0$  two zones can be singled out: a middle part of a liner and a wall one. In a middle part a shape of a liner is close to that of a cylinder ( $\alpha = 0^\circ$ ).

In the wall zone movement is very instable. It is observed that liner ends could be ahead its middle part ( $\Delta r/r \sim 0,2$ ) or they could be behind it ( $\Delta r/r \sim 0,5$  or  $\Delta r/r \sim 1$ ), or a liner could lose contact with a wall, or metal could deposit on electrodes.

Perturbation zone extends at an angle of  $\beta = 25^\circ$  from the wall. " $\beta$ " is very instable and evidently depends on the "quality" of a joint: liner - wall.

When a connection with a wall is "joint" (experiment N2) at a radius of 0,25  $R_0$  a middle part of a liner moves as a cylinder free of any noticeable perturbations. At an angle of  $\alpha = 3^\circ$  a picture is very favorable. Practically there are no perturbations near walls. At  $\alpha = 0^\circ$  a liner completely loses contact with walls along the whole perimeter, making a gap, which corresponds to  $\beta$  from  $35^\circ$  to  $40^\circ$ , i.e. "joint" instability manifests itself again.

The value of radial lags near a gap reaches  $\Delta r/r \sim 0,7$ .

For a middle zone radii of liners at the moment of radiography match well with the results of 1-D calculations.

The largest perturbations in the zone of "joint" are observed, when walls are straight ( $\alpha = 0^\circ$ ), when a liner is located "jointly" to a wall. Even in the case with straight walls, when the connection is sliding with overlap of only 0,5 mm, it works better. That means that in future experiments the value of overlap should be increased. A small incline of the walls ( $\alpha = 3^\circ$ ) brings to further decrease of perturbations.

In order to decrease wall perturbations it is interesting to observe their development, when a liner comes tightly to a wall (either with a larger value of the overlap or with "joint" free connection).

It was even more interesting to evaluate the stability of the results, when the experiment was repeated the same way (similarly to experiment N2).

We have also prepared and conducted the third and the forth experiments.

Technical representative of VNIIEF  
Professor

28.12.94

*V.K. Chernyshev*  
*Ye.I. Zharinov*

V.K. Chernyshev  
Ye.I. Zharinov

The repetition of experiment N2 without significant changes showed (see exp. N3) that the opinion, made earlier about the advantage of slightly inclined walls ( $\alpha = 3^\circ$ ) comparatively to straight walls ( $\alpha = 0^\circ$ ) in case, when liners are located "jointly" to the walls, is not confirmed. At  $\alpha = 3^\circ$  a liner completely lost contact with the wall along the whole length of a perimeter, and a gap was formed, which had an equal angle and the dimension equal to two liner thicknesses, but only from one liner end for incomprehensible reason.

Parts of a liner adjacent to a gap lagged behind by  $\Delta r/r \sim 0,1$ . The other liner's end flew normally.

At  $\alpha = 0^\circ$  a liner did not leave walls from none of the ends. Close to walls one can see that liner's ends are a little ahead the middle part not more than  $\Delta r/r = 0,15$  in a zone  $\beta = 20^\circ$ .

Experiment N 3 confirmed strong dependence of perturbation picture on very small changes in initial conditions which earlier were not controlled, probably, as a result of difference in gaps along the liner perimeter, measured in microns, when connection is "joint". The issue arose about more reliable connection between a liner and walls for sure free of gaps.

It was interesting to watch the character of wall perturbations, when the liner's overlap was increased twice ( up to 1 mm ) and at the same time radial tightness of 15 microns was used.

With that aim the character of liner movement in a wall zone was specified. To estimate stability of the phenomenon the liner was accelerated under three absolutely similar initial conditions ("overlap" was 1 mm, tightness - 15 microns,  $\alpha = 0^\circ$  and  $\alpha = 3^\circ$ ).

Technical representative of VNIIEF  
Professor

28.12.94 *В. К. Чернышев* V.K. Chernyshev

*Я. И. Жаринов* Ye. I. Zharinov

ABSTRACT  
Contract F 61708-94- C-0014  
Item 003

The experiments with three liners (experiment N 5 and experiment N 6 ), which were conducted similarly ("overlap" is 1 mm, tightness is 15 microns,  $\alpha = 0^\circ$  and  $\alpha = 3^\circ$ ) at the moment, when  $R/r_0 = 0,5$ , confirmed that:

- liner does not lose contact with a wall ( even with  $\alpha = 0^\circ$  )
- lack sparp of splashes of liner metal, being observed earlier (both inside or outside) near the wall
- presence of little ( $\Delta r/r < 0,05$ ) smooth perturbations in the zone  $\beta = 30^\circ$  for both straight and slightly inclined ( $\alpha = 3^\circ$ ) walls.

All the conducted experiments again put forward the issue how much regular the good result was, which was obtained in the experiment N 2 with  $\alpha = 3^\circ$ .

To answer this issue experiment N 2 was repeated ( see exp. N6) for straight walls, which make more perturbations. Thickness of a liner was decreased up to 0,7 mm, in order to observe the beginning of expansion in a middle zone. At  $\alpha = 3^\circ$  thickness of a liner was preserved.

Radiography made at a moment, close to a moment of focusing, showed that, when  $\alpha = 3^\circ$  liner also lost contact with walls at both ends, wall perturbations highly increased ( up to  $\Delta r/r \sim 1$  ).

Hence, the ways to minimize wall perturbations have become clear.

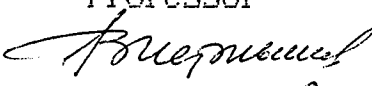

Development of perturbations is very complicated and interesting, it depends on small changes of initial conditions. All this makes the following comparison of results of 2 - D numerical calculations, in which Fillips Lab has achieved significant progress, with the future experimental data very encouraging.

1-D calculations, made for a middle part of a liner length, showed that at the radius of  $\Delta r/R_0 \sim 0,1$ , the velocity of inner liner shell is 5,4 km/sec for the initial thickness of 1,0 mm and 7,6 km/sec - for the thickness of 0,7 mm.

We evaluated the temperature at the moment of liner implosion.

We also have finished the analysis of experimental and computational data and have written the final report " Study of Imploding Electrode Wall Interaction" under the contract F 61708-94-C-0014.

Technical representative of VNIIEF  
Professor

28.12.94  V.K. Chernyshev  
 Ye. I. Zharinov

Abstract	3
Introduction	4
1. Description of experimental scheme	5
Methods of measurements	5
2. Description of a liner system	13
3. Results of experiments ;	16
their comparison with calculations	16
4. Discussion of experimental results	43
Conclusions	47
References	48

## ABSTRACT

The report gives the results of the experiments on aluminum liner acceleration and their interaction with electrode walls. The liners having the radius of 30 mm, wall thickness of 1 mm and 0,7 mm and a length of 30 mm are accelerated by a magnetic field, created by explosive magnetic generator (EMG). A helical generator 100 mm in diameter and 700 mm in length was used to create a magnetic field. During the process of compression a liner shape was recorded using X-ray facility.

The report gives experimental set - up, electrical and design data of experimental units and diagnostical equipment and also raw experimental data, analysis data and description of an analysis method.

Based on the experiments we chose the method to bring a liner into a contact with electrode walls, which permits continuous contact of a liner with electrode walls in the process of motion.

The work is done under the contract "Study of Imploding Liner - Electrode Wall Interaction" ( N F 61708 - 94 - C - 0014), made between the "Phillips Lab" (USA) and VNIIEF (Russia).

## INTRODUCTION

The report gives the results of experiments and calculations made at VNIIEF under the contract N F61708 - 94 - C - 0014, made between "Phillips Lab" (USA) and VNIIEF (Russia) in 1994. The issue of interaction between solid liners, accelerated by the magnetic field, and the end electrode walls is of great interest for both laboratories.

Acceleration of solid liners which do not explode during the flight is widely used to obtain ultra - high magnetic fields, to compress plasma, to study the properties of various materials under high magnetic pressure and etc. /1-4/.

When a liner interacts with electrode walls the following phenomena can appear: advance or lag of liner boundaries (azimuthal and axial asymmetry), melt and evaporation of liner material, local distortions of a shape, etc.

These phenomena depend on magnetic field voltage, strength properties of a liner and electrodes, angle of electrode walls slope and other reasons.

The main goal of the experiments was to define the picture of interaction between aluminum liners of various thickness and electrode walls. Aluminum liners with 30 mm radius and 30 mm length were subjected to study. To receive more information during experiments we used a liner system (LS) consisting of two independent liners, which enables us to record a liner position at a given instant with one and the same discharge current.

As an energy source we used a helical explosive magnetic generator (EMG) with 100 mm in a diameter and 0,7 m in length, having effective operation time of 15-17  $\mu$ sec which produces currents in LS up to 5,9 MA.

The shape of liners at various stages of movement was recorded using an X - ray facility. Time of exposure was from 50 to 70 nsec.

Six explosive shots were conducted with a liner system. The representatives of Phillips Lab were present at first two shots.



# 1. DISCRIPTION OF EXPERIMENTAL SCHEME. METHODS OF MEASUREMENTS.

Fig.1.1 shows the scheme to conduct explosive shots to accelerate cylindrical liners by the magnetic field, created using an explosive magnetic generator.

The main components are : a liner system (LS), which is under investigation; a helical explosive magnetic generator (EMG), which is the source of energy for LS ; a capacitor bank (CB) with an energy source of 0,5 MJ, which is a source of energy to power an EMG; X - ray facility; high-voltage units HU-19-I and HU-19-II to fire EMG and trigger an X-ray facility ; time-delay units for pulse triggers DU-1 and DU-II ; a set of measuring equipment to record the main electric EMG characteristics.

The detailed description of LS is given in the next section.

A helical EMG of 100 mm diameter and 700 mm length was used as a source of energy. EMG provided current pulses in LS with a characteristic rise - time from 15 to 17  $\mu\text{sec}$ , which provides currents in LS up to 5,9 MA. The full time of generator operation was 85  $\mu\text{sec}$ .

Fig.1.2 shows EMG together with the liner system.

A capacitor bank is able to store 1200 $\mu\text{F}$  and charge voltage up to 30 kV to power EMGs. In our shots we used only a part of a 480 $\mu\text{F}$  capacitor bank, which was charged up to the voltage of 15 kV. The store of energy was enough to provide the required current for EMG powering.

The powering current and current derivatives in EMG were measured using Rogovsky coil and inductive probes of various sensitivity. Probes were located in a cavity of LS casing at equal distances from the system axis. An inductive probe is a coil of small dimensions, winded by an insulated wire ( $\varnothing$  0,28 mm) into dielectric frame out of plexiglass of a given cross - section (6 $\times$ 6 mm<sup>2</sup>). To reduce parasitic noise from the external field the coil output ends were bifilar. The coil was installed into a plexiglass casing, filled by insulating compound to increase electrostrength

# Arrangement of an explosive shot

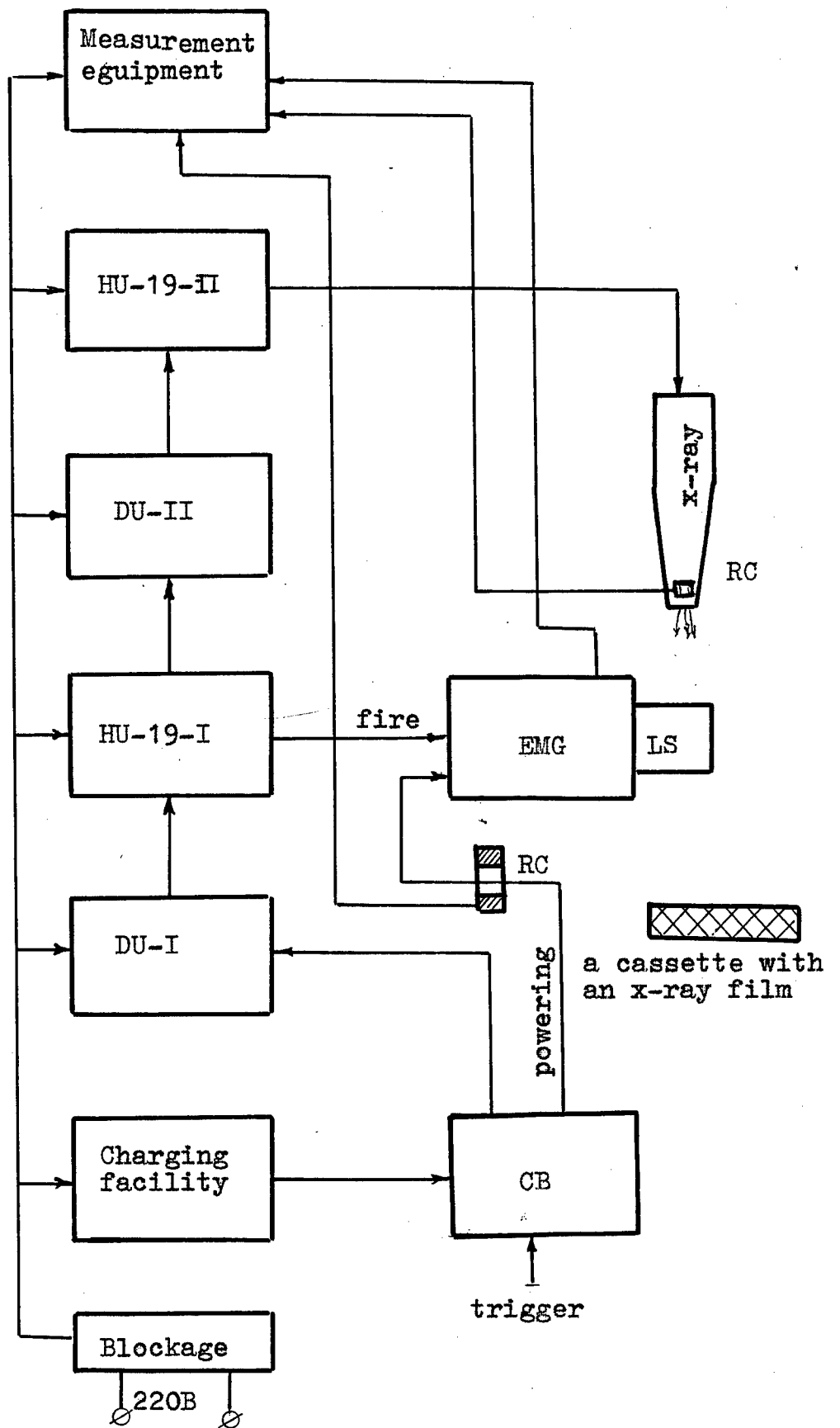


Fig.I.I

EMG with a liner system

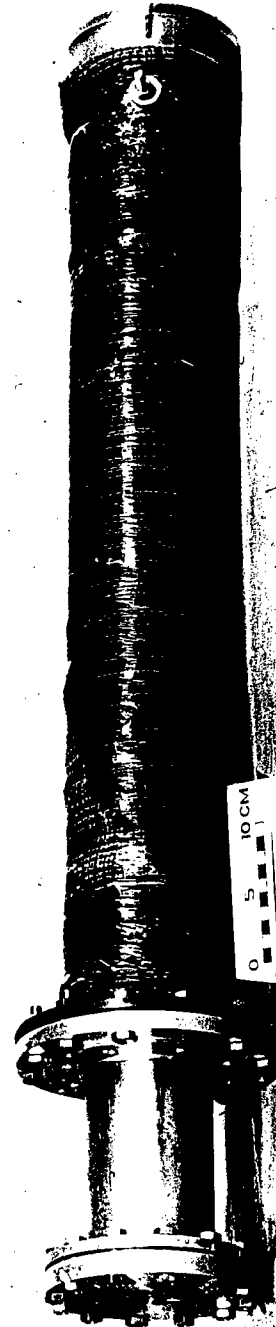


Fig. 1.2

and protection from liner explosion products.

Fig.1.3 shows the measuring unit with eight probes. The number of turns in inductive probe coils was from 100 to 4 to record current derivative from  $10^{10}$  A/s at the beginning of EMG operation to  $3 \cdot 10^{11}$  A/s at the end of its operation.

Voltage pulses from inductive probes were applied directly to vertically deviating plates of two - beam oscilloscopes and were recorded from screens into photofilm. Voltage amplitudes from probes reached several hundred volts.

The state and position of liners at a given instant were recorded using X-ray facility, including the following main units:

- pulse voltage generator (PVG),
- opening switch,
- charge facility,
- control desk,
- vacuum system,
- vacuum diod.

The X-ray facility is given in Fig.1.4.

The main characteristics of an X-ray facility are:

energy stored in a pulse voltage generator	is 5 kJ,
output voltage	is 0,5-1 MV,
PVG capacity under discharge	is 20 nF,
inductance in a discharge circuit	is $7 \mu\text{H}$ ,
limiting residual pressure	
in a chamber of a vacuum diod	is $10^{-3}$ Pa ( $10^{-5}$ torr),
X-ray radiation dose at the	
distance of 1 m per pulse	is 1-1,5 R,
X-ray pulse duration	is 50-70 nsec.

Rogovsky coil was used in a PVG discharge circuit to record the moment, when x-ray radiation appears. The pulse from Rogovsky coil was applied to the second beams of oscilloscopes, which record EMG current derivatives.

The components operate in the following way.

First of all the capacitor bank is charged up to the required value using a charging device. Upon the order "Trigger" a capacitor bank is discharged on the helical EMG coil. At the same time using the DU-1 pulse delay unit, HU-19-I high - voltage unit is triggered,

A measuring unit with inductive probes

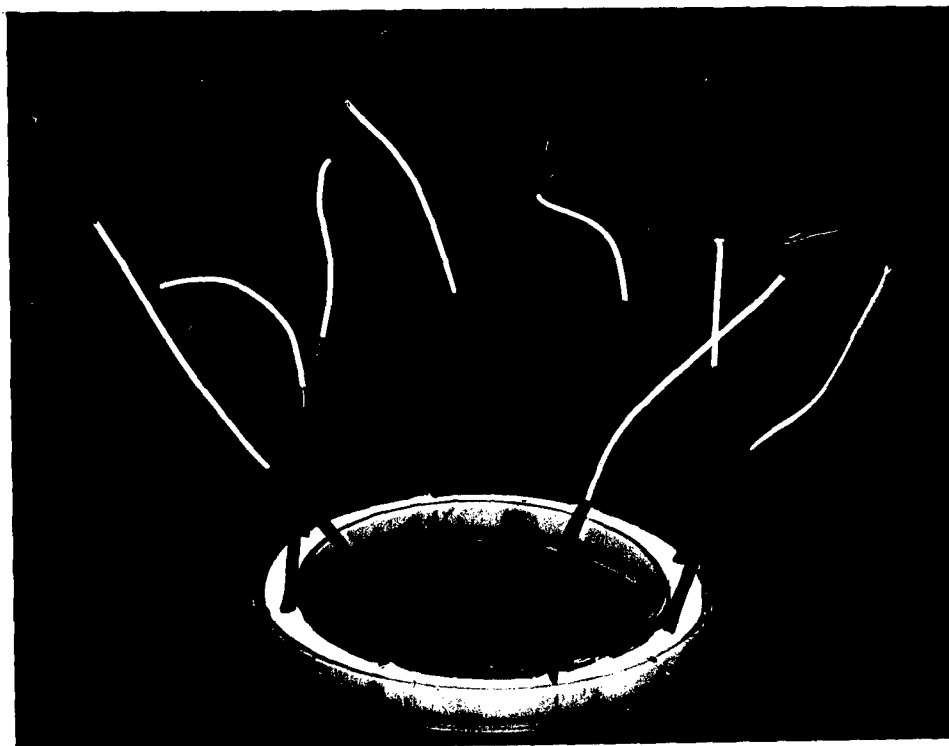


Fig. 1.3

## X-ray facility

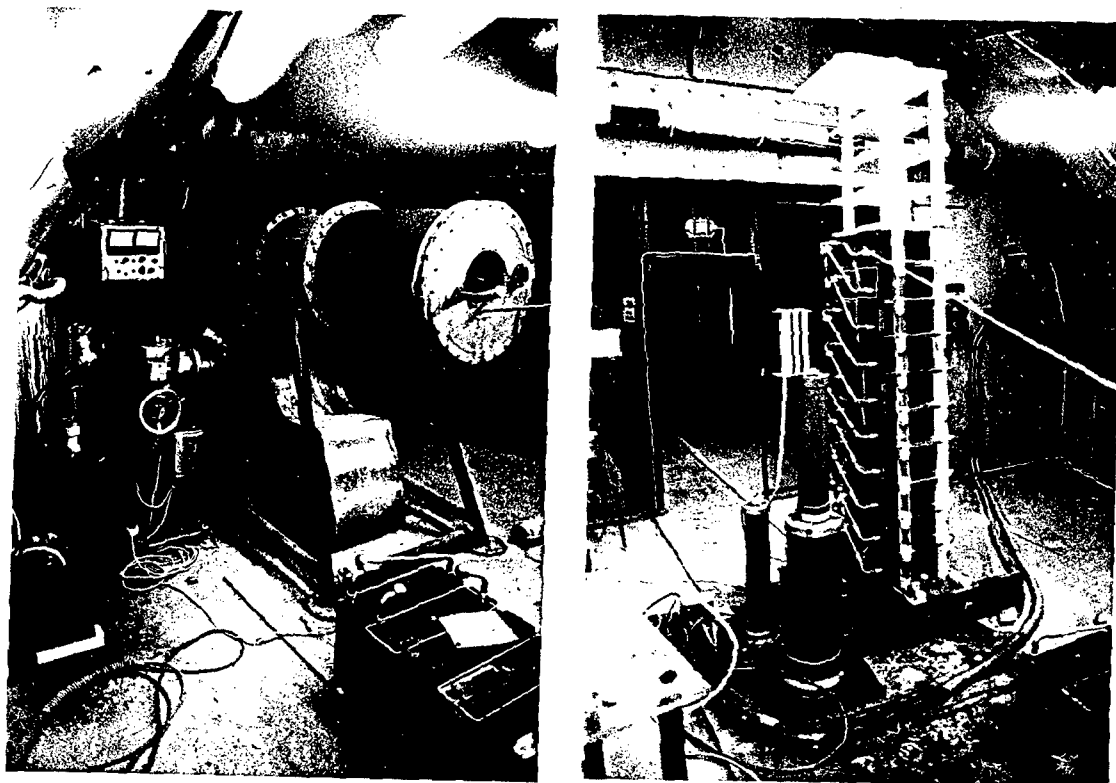


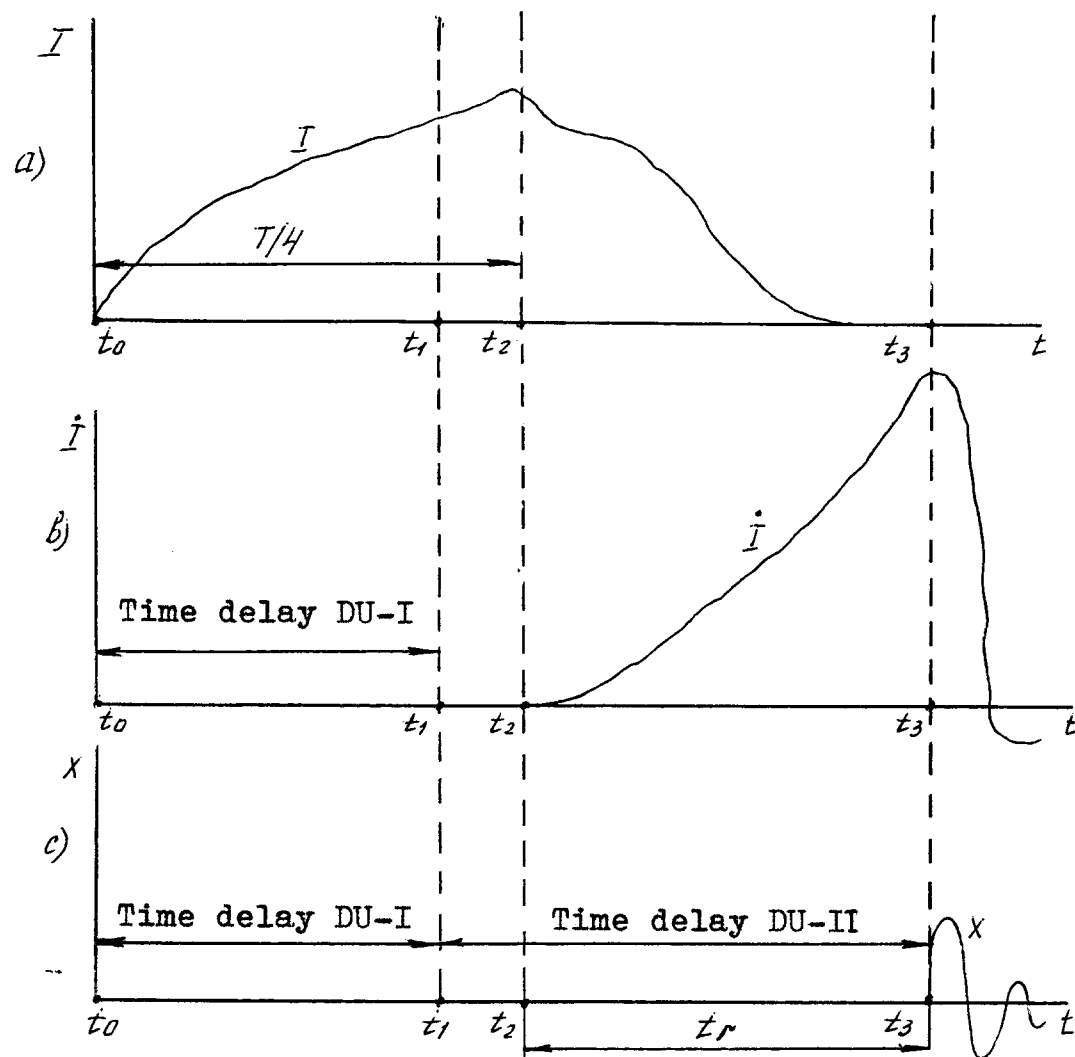
Fig. 1.4

which provides detonation of the HE charge electrodetonator in an EMG tube. Using the same pulse, HU-19-II high - voltage facility is triggered, which provides triggering of x - ray facility.

DU-1 time delay unit was adjusted in such a way that to the moment, when helix turns began to deform (when EMG current started to increase), the current from a capacitor bank would reach its maximum. Delay time to trigger BY-19-II and an x - ray facility was chosen keeping in mind the moment of LS radiography.

Time diagrams of EMG powering currents, current derivatives of EMG and x - ray pulse are plotted in Fig.1.5.

Time diagram of EMG powering currents,  
EMG current derivative and x-ray pulse



Designations:

- $I$  is EMG powering current, recorded by Rogovsky coil (RC) ;
- $\dot{I}$  is current derivate in an EMG and LS, recorded using inductive probes ;
- $X$  is voltage pulse from RC of x - ray facility Rogovsky coil;
- $T/4$  is quarter of period of the capacitor bank discharge into EMG inductance;
- $t_0$  is beginning of the capacitor bank discharge ;
- $t_1$  is the moment of electrodetonator firing in an EMG ;
- $t_2$  is the moment, when EMG helix starts to deform ;
- $t_3$  is the moment, when a voltage pulse from RC of x-ray facility appears ;
- $t_r = t_3 - t_2$  is time of radiography.

Fig. 1.5



Study of interaction between liners and electrode walls, defining of their flight symmetry was carried out on a liner system (LS), which is schematically shown in Fig. 2.1.

To receive more information from the shot we developed a double liner system, which enables to observe simultaneously the flight of two independent liners (with one and the same EMG discharge current).

LS represents a coaxial facility, consisting of two cylindrical liners (1) and (2), located between lateral electrodes (3) and (4) and a central electrode (5), dividing LS into two independent portions; a massive outer casing (6) and an insulator (7). In some assemblies in order to achieve uniform current spreading we put a cylinder (8) made of aluminum foil above the liners. The foil thickness was 0,045 mm, its ends were lap-connected with electrode walls. The connection between liners themselves and electrodes was either "overlapping" or "joint".

Position (9) denotes location of inductive probes.

An outer casing (6) with a wall thickness of 10 mm was made of aluminum alloy, AMZ. This enabled to achieve sufficiently good liner pictures using radiography though they were located inside the metallic casing.

An insulator of 2 mm thickness was made of mylar.

In the first experiments liners and electrodes in LS were made of aluminum alloy, AMZ. For the following experiments we chose more refractory metal, steel, for electrodes and aluminum (mark A 995), the metal with more conductivity and practically without impurities, for liners.

Electrode walls were made both flat or conical shapes with a slope angle up to  $3^\circ$ .

The liner system as an assembly or as separate units is shown in Fig. 2.2.

Liner system

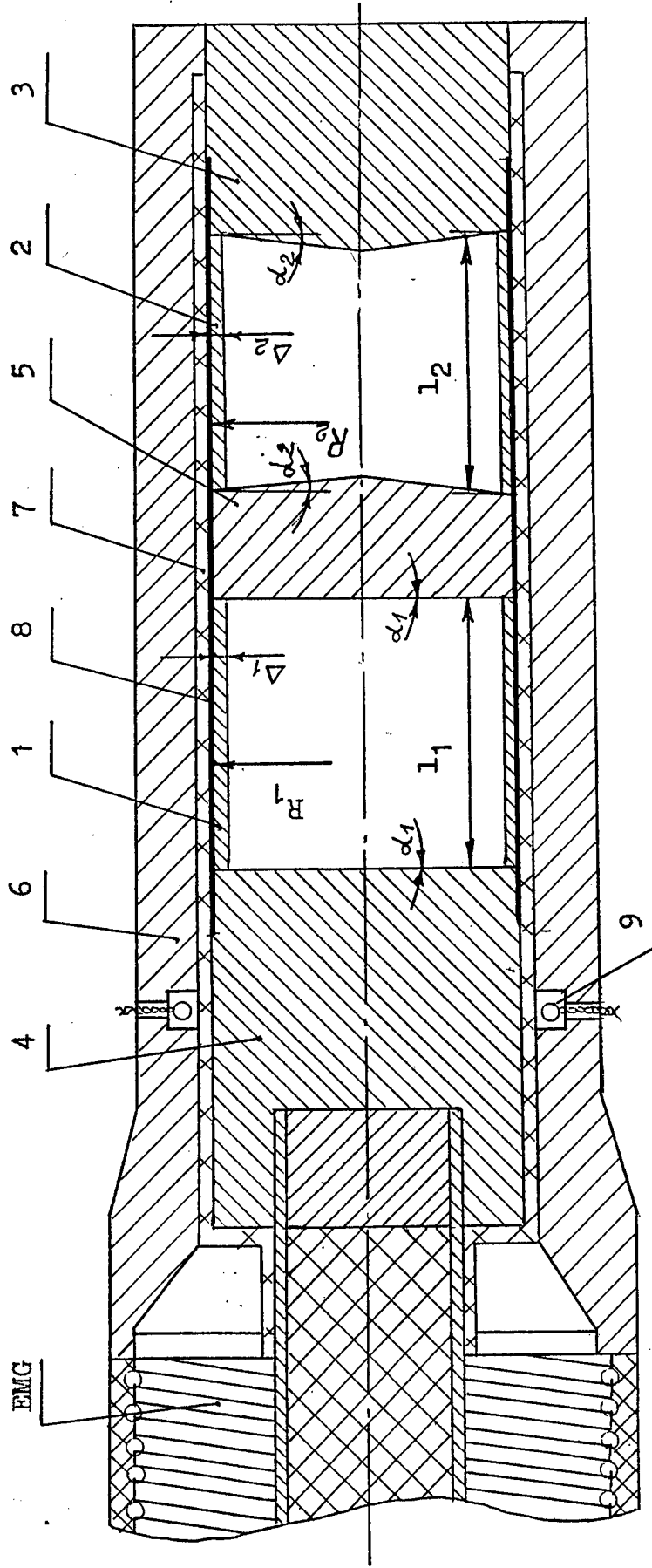


Fig.2.1

Liner system as an assembly or as  
separate components

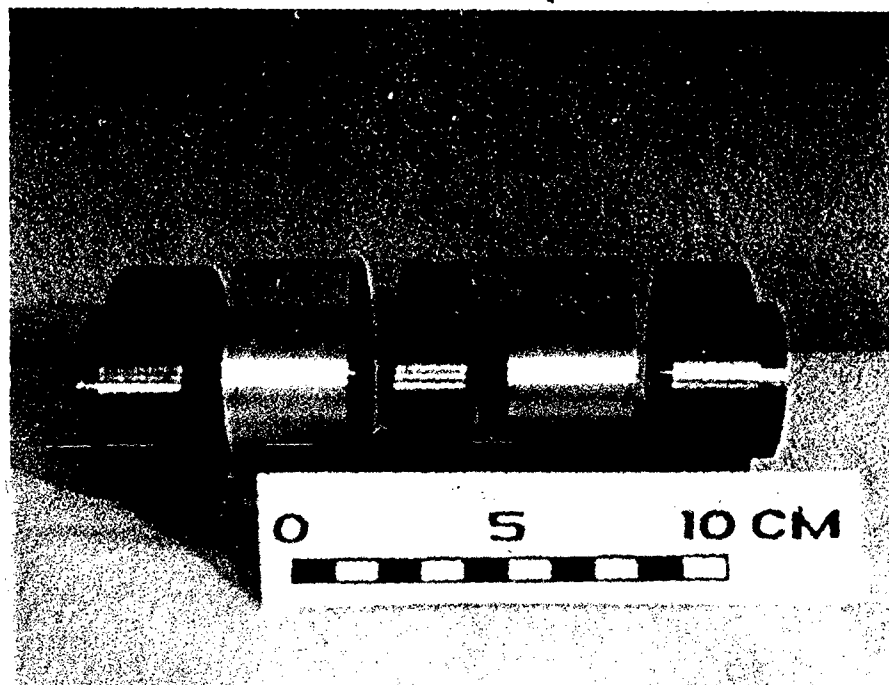
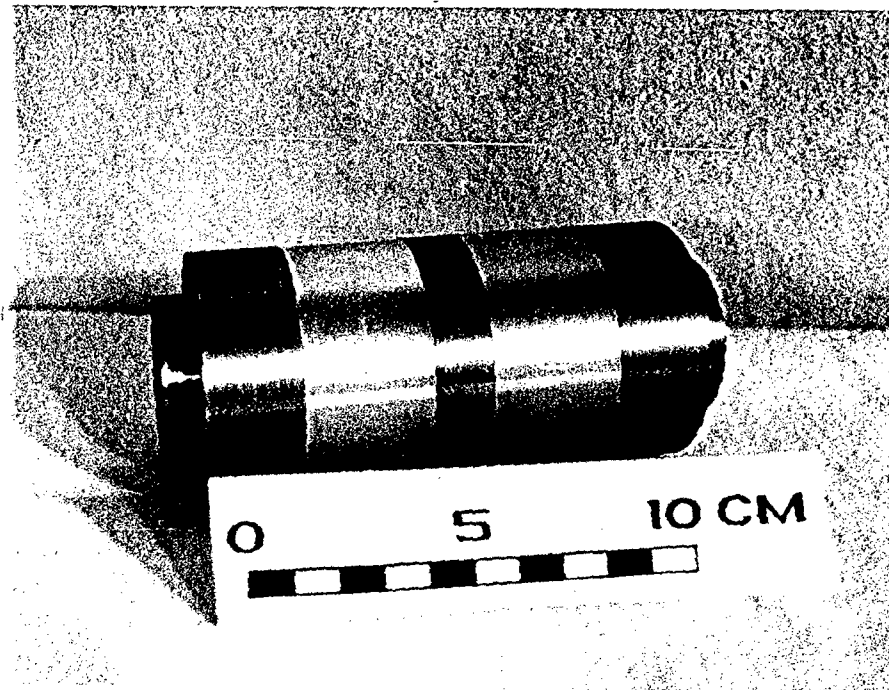


Fig. 2.2

### 3. RESULTS OF EXPERIMENTS ; THEIR COMPARISON WITH CALCULATIONS

Two sets of explosive shots were conducted using liner systems. The external radius of liners was 30 mm, wall thickness was 0,7 mm and 1 mm, length was 30 mm. The goal of experiments was to study a liner shape and its interactions with electrode walls. Based on these studies we tried to choose a method to connect a liner with walls with which the continuous contact could be provided.

In the first set of four shots the liners of aluminum alloy, AMZ (2,73 g/cm<sup>3</sup> density,  $2,86 \cdot 10^5$  1/ohm·cm conductivity, 654°C melting temperature) were tested /5/. Electrodes were made of the same alloy.

In the second set of two shots we tested liners of A 995 aluminum with 2.7 g/cm<sup>3</sup> density,  $3,77 \cdot 10^5$  1/ohm·cm conductivity and 660°C melting temperature. Electrodes were made of steel (mark 30).

The radius of compression and liner flight velocity, the current effect integral  $Y = \int_0^t I^2 dt$  and double current effect integral  $Z = \int_0^t \int_0^t I^2 dt dt$  were calculated in the experiments, by 1-D MHD code with the given equation of state and aluminum conductivity /6/. The comparison of the experimental data and calculation was made.

#### THE FIRST SET OF EXPERIMENTS

##### SHOT 1

The design of a liner system with the main dimensions is shown schematically in Fig.3.1. The left liner was located between flat electrodes, the right one - between conical electrodes with slope angle of 3°. Both liners were mounted on electrode plateau (0,5 mm) by their overlapping ends and had a loose fit over the diameter.

LS radiograph made at the instant  $t_p = 74,2 \mu\text{sec}$  from the beginning of current appearance in liners is given in Fig.3.2.

Fig.3.3 (a) gives oscillograms of EMG powering current (the first upper beam) and EMG current derivative (the second low beam), recorded by a probe, having 30 turns. The oscillograph started to

Shot 1  
LS design

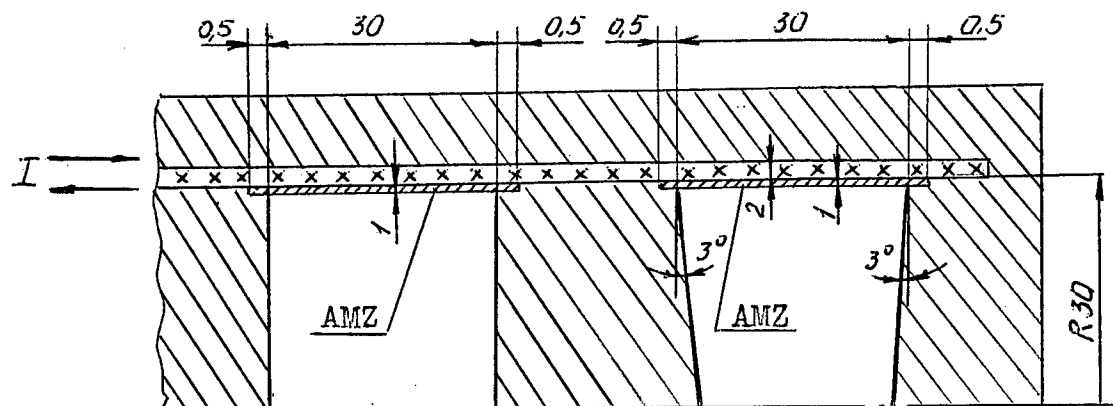


Fig. 3.1

Radiograph

(working picture -  $t_r = 74,2 \mu\text{sec}$ )

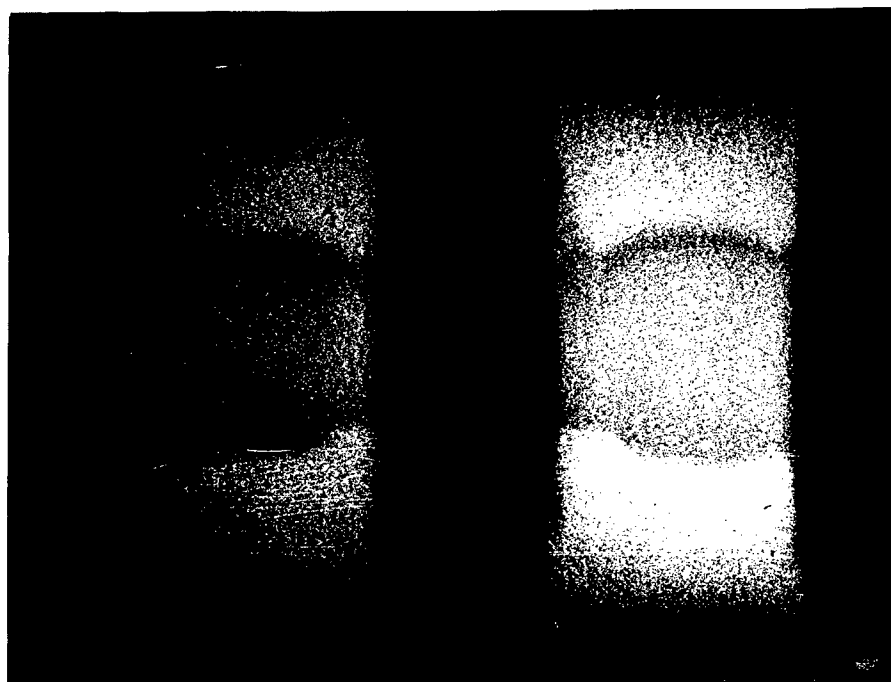
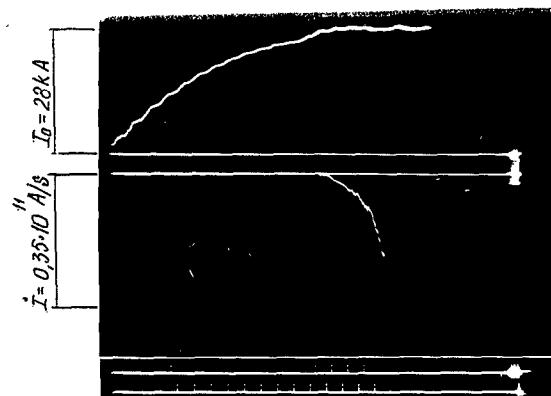
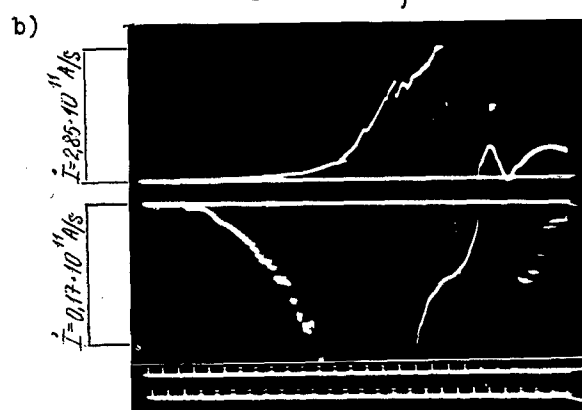


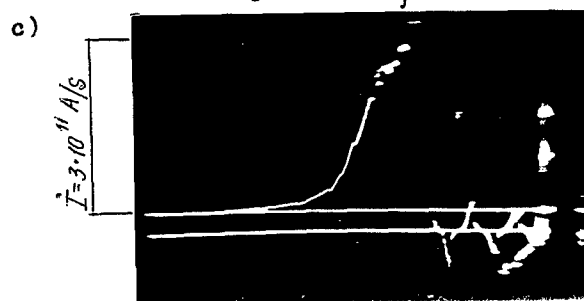
Fig. 3.2



1 point = 4  $\mu\text{sec}$



1 point = 4  $\mu\text{sec}$



pulse from RC

Shot 1

EMG current dependence on time

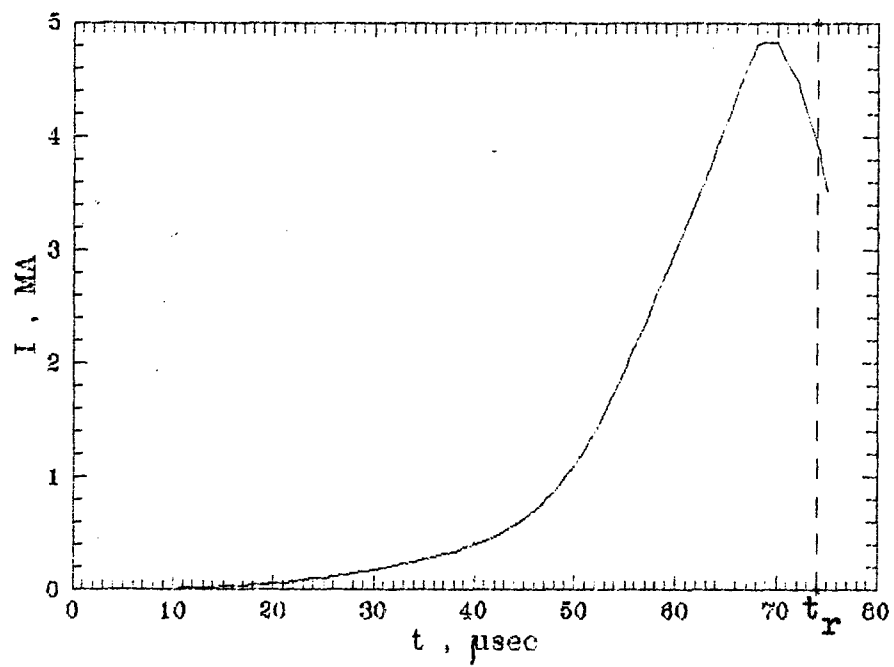


Fig. 3.4

Dependence of liner radius on time

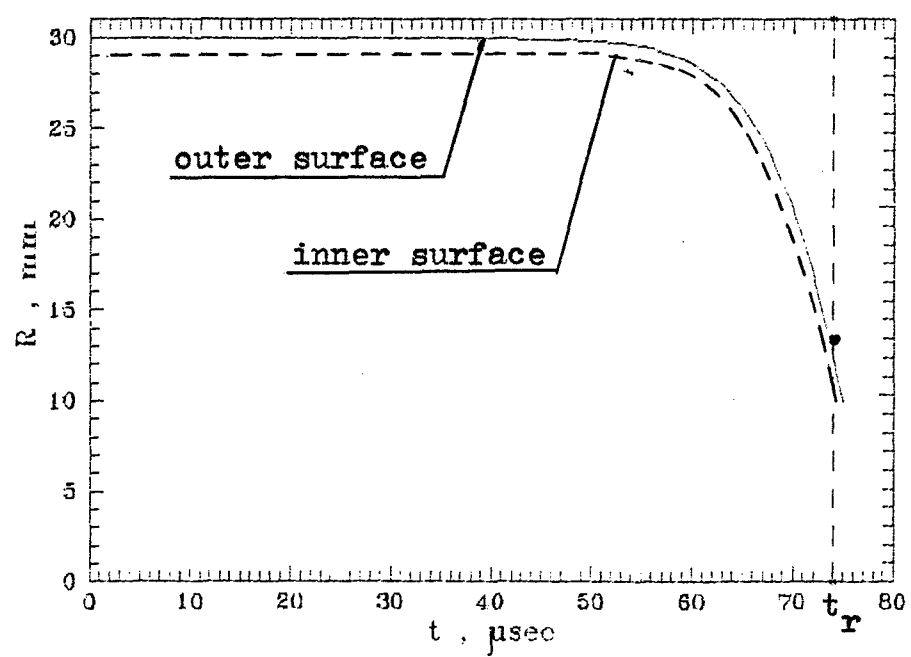


Fig. 3.5

operate simultaneously with capacitor bank discharge.

Fig.3.3 (b) and 3.3 (c) give oscillograms of EMG current derivatives from probes having 100 turns and 6 turns, correspondingly. The second oscillograph beams (Fig.3.3 c) recorded pulse from RC of x - ray facility at the moment of radiation.

The pictures also show time sweep with time marks.

All the oscillographs, recording EMG current derivatives from the probes of various sensitivity, including those, which oscillograms are not given here, were triggered by HU-19-I.

EMG powering current ( $I_0$ ), at the moment, when helix turns deform is calculated by the formula :

$$I_0 = \frac{N_c \cdot U_0}{R_{sh}} \quad (A),$$

where :  $N_c$  is a number RC turns,

$U_0$  is voltage on an oscillograph, V

$R_{sh}$  is resistance of a shunt, Ohm.

EMG current derivatives ( $\dot{I}$ ) were calculated according to the formula :

$$\dot{I} = \frac{5 \cdot 10^8 \cdot U \cdot R_0}{N \cdot S} \quad (A/s)$$

where:  $U$ ..... is voltage on an inductive probe, V ;

$N$ ..... is number of probe turns ;

$S = 0,394 \text{ cm}^2$  is the square of a single turn ;

$R_0 = 5,75 \text{ cm}$  is a radius from the turn center to the axis ;

$5 \cdot 10^8$ ..... is constant coefficient.

EMG current derivatives according to probes of various sensitivity were averaged.  $I(t)$  current curve was plotted according to averaged dependence,  $\dot{I}(t)$ , by integration.

As it is seen from a radiograph (Fig.3.2) central liner parts have been moving along the radius sufficiently symmetrically. No noticeable perturbances or non - uniformities were seen on the outer surfaces. No noticeable difference in behaviour of a liner, located



between straight and conical electrodes was discovered.

At the moment of radiographing the radius of liner central parts along the outer surface in average was  $R_r = 0,43R_o = 12,9$  mm.

The perturbation of the ends in the wall areas in both liners is observed. The ends of the right liner, located between conical electrodes are ahead of the central part from both sides. From the left side one can observe the initial stage, when the liner end leaves the electrode wall. The right end of the left liner, located between the electrodes with straight walls, also is ahead of the central part. The liner practically completely leaves the electrode wall in the left wall area.

Peak EMG current derivative was  $3 \cdot 10^{11}$  A/s.

Fig. 3.4 presents EMG current dependence on time, obtained by integration of current derivative in shot 1. The same picture shows the moment of tr liner system radiography.

Peak current in a liner system was  $I_{max} = 4,9$  MA, to the moment of radiography it decreases to the  $I_r = 3,9$  MA. Current effect integral at the tr moment was  $Y_r = 2,98 \cdot 10^8$  A<sup>2</sup>·s,  $Z_r = 2,5 \cdot 10^3$  A<sup>2</sup>·s<sup>2</sup>.

Estimated dependendce of a liner radius on time, obtained by 1-D MHD code for experimental EMG current dependence in shot 1, is shown in Fig. 3.5. In the same Fig. one can see a point, which denotes the radius of the outer liner surface, obtained in the experiment (tr moment), which practically matches the calculation data.

## SHOT 2

In this shot LS design (Fig. 3.6) distinguished from LS design in the shot 1 only by the fact that the liner ends, which are "joint", came across electrode walls, the cilinder of aluminum foil 0,045 mm thick was put above the liners. The cilinder came tightly across the liner surface, its ends were squeezed between an electrode and a casing.

We conducted the experiment aiming to define a shape and character of interaction between a liner and the walls at the later stage of their movement.

Shot 2  
LS design

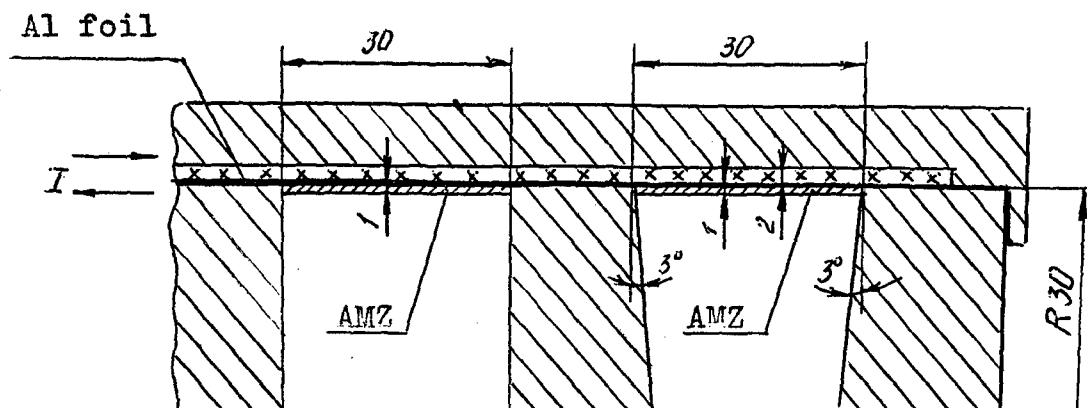


Fig. 3.6

Radiograph  
(working picture -  $t_r = 76,6 \mu\text{sec}$ )

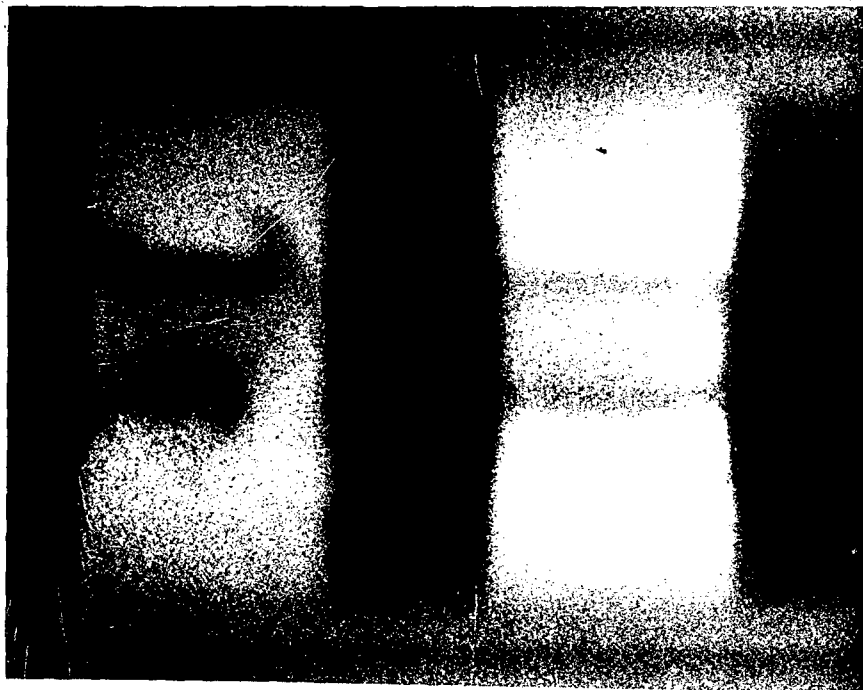
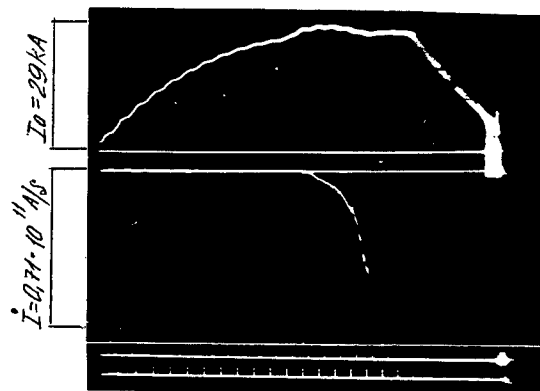
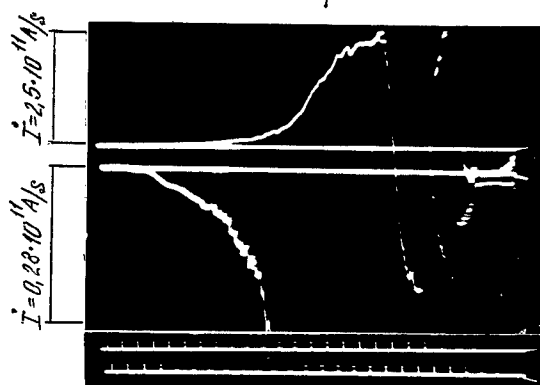


Fig. 3.7

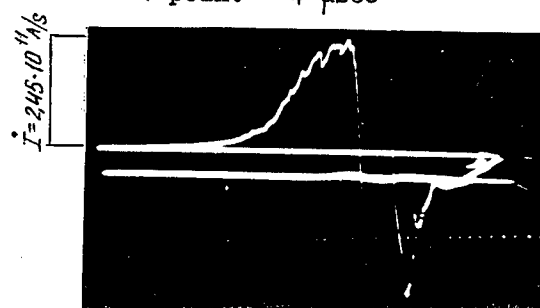
a)



b)



c)



EMG current dependence on time

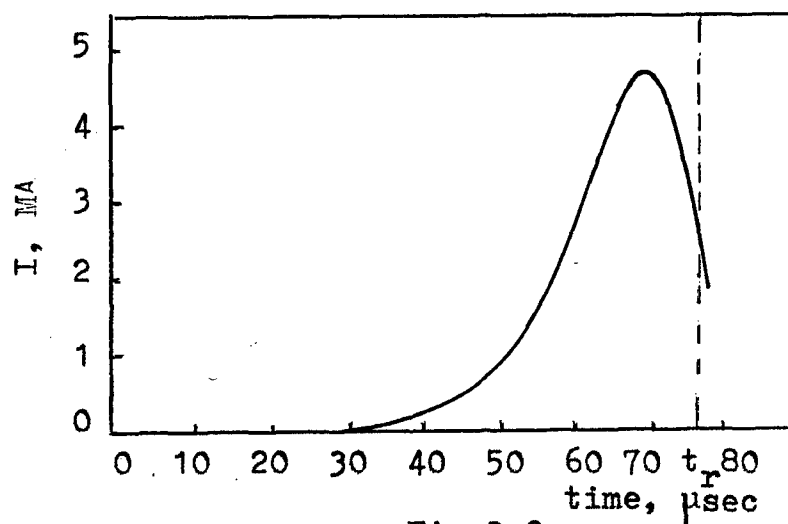


Fig.3.9

Dependence of liner radius on time

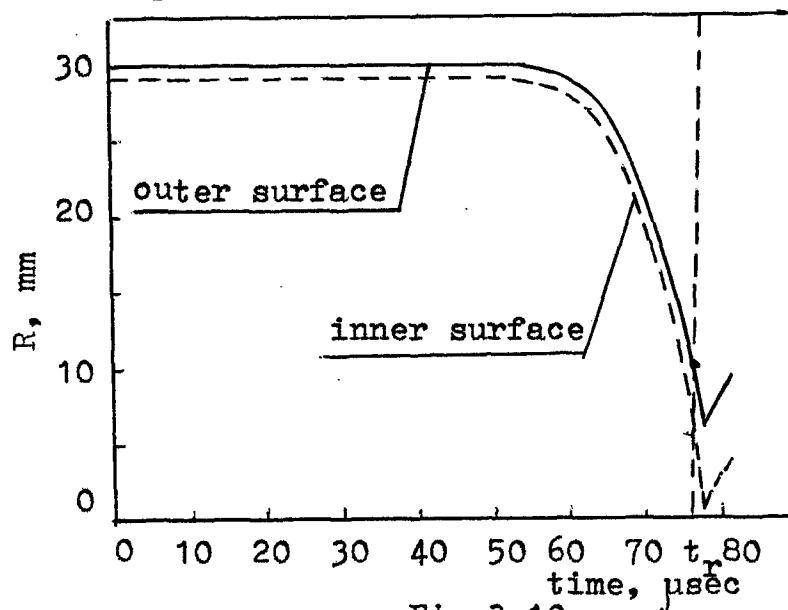


Fig.3.10

Dependence of liner velocity on time

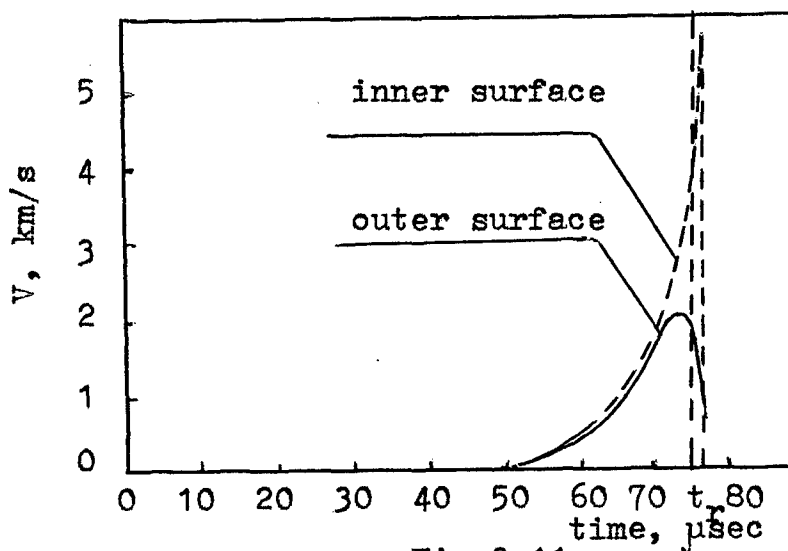


Fig.3.11

Fig. 3.7 shows LS radiograph made at  $t_r = 76,6 \mu\text{sec}$ . Oscillograms of EMG powering current, EMG current derivatives are given in Fig. 3.8 (a,b,c). As it is seen from a radiograph (Fig. 3.7) the picture of interaction between liners and walls comparatively with shot 1 has changed significantly. The ends of a left liner, located between flat electrodes practically along the whole perimeter blew up and separated from the walls.

A right liner located between conical electrodes flew close to the axis with a symmetry good enough. A good contact of liner ends with electrode walls has been retained.

The appearance of local depressions on the surface of flat electrodes was unexpected for us (Fig 3.7). They are, probably, the result of metal burning under the effect of electric explosion.

EMG current dependences on time, are given in Fig. 3.9.

From the experiment the following is obtained:

$I_{\text{max}}=4,7\text{MA}$ ,  $I_r=2,9 \text{ MA}$ ,  $Y_r=2,9 \cdot 10^8 \text{ A}^2 \cdot \text{s}$ ,  $Z_r=2,8 \cdot 10^3 \text{ A}^2 \cdot \text{s}^2$ ,  $R_r=0,33 R_o=10\text{mm}$ .

Estimated dependences of radii and liner velocities on time are given in Fig. 3.10 and 3.11. These pictures show the moment of radiography  $t_r$ . The point in Fig. 3.10 shows the radius of an outer liner surface obtained in the experiment.

### SHOT 3

From the point of view of the design shot 3 (Fig. 3.12) was the repetition of shot 2. Its goal was to verify the results of shot 2, where a liner, located between conical electrodes, came up to the axis with the symmetry good enough. But our hopes have not come true in the experiment.

Fig. 3.13 shows LS radiogram at the moment of  $t_r = 77 \mu\text{sec}$ . As it is seen from a radiograph liners are at the earlier flight stage, though the right liner located between conical electrodes, has already separated from the left end. The reason for that is mostly likely the poor contact between the left liner end and the electrode wall. The ends of the left liner continue to be in continuous contact with the flat walls, but in the area of contacts the ends of the liner are significantly ahead of the central part.

Shot 3  
LS design

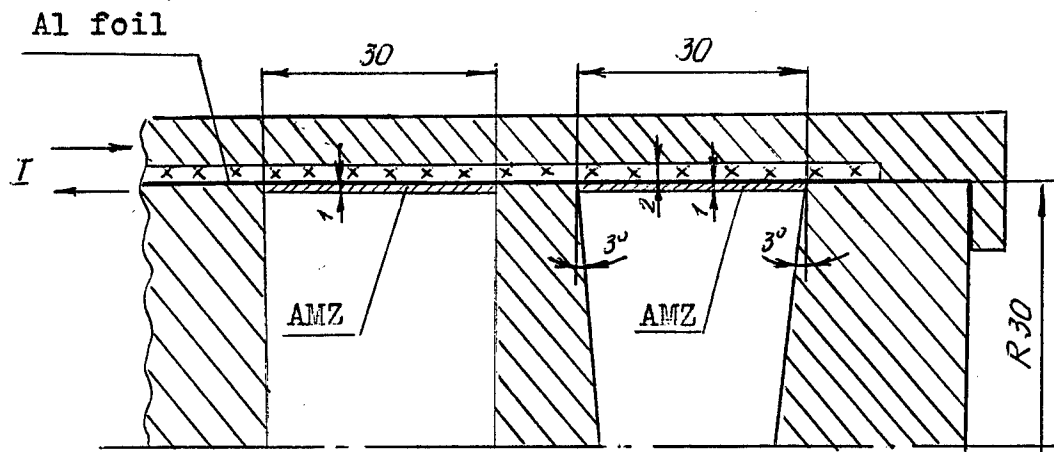


Fig. 3.12

Radiograph

(working picture -  $t_r = 77 \mu\text{sec}$ )

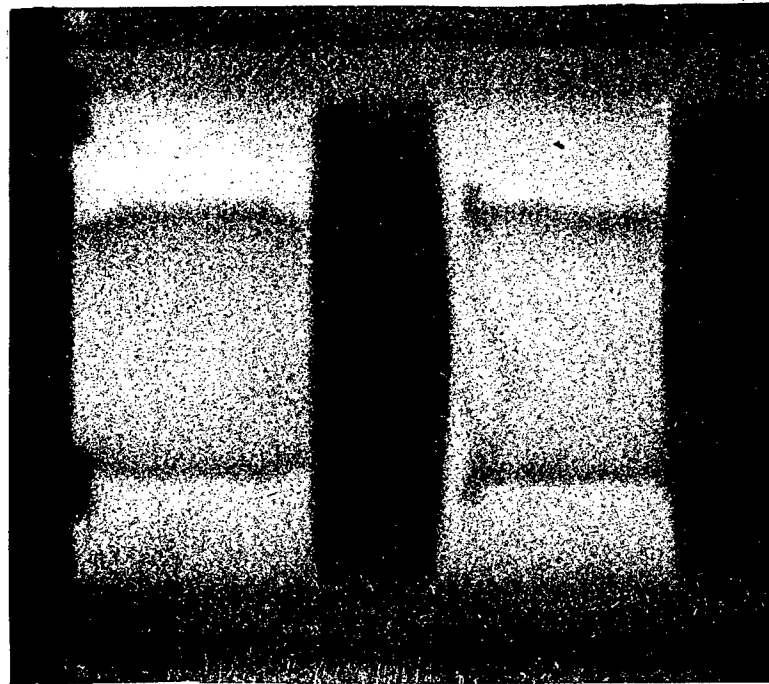
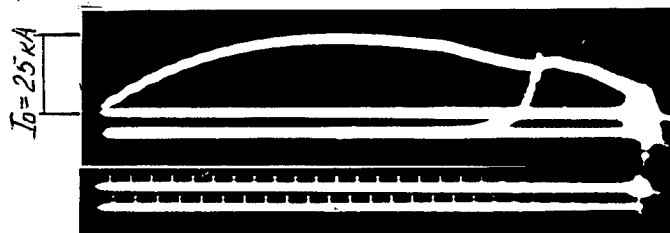


Fig. 3.13

Shot 3  
Oscillograms

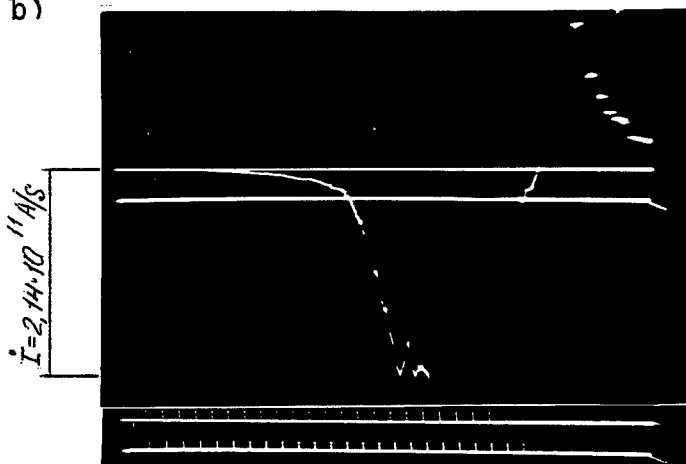
1 point = 10  $\mu$ sec

a)



1 point = 4  $\mu$ sec

b)



1 point = 4  $\mu$ sec

c)

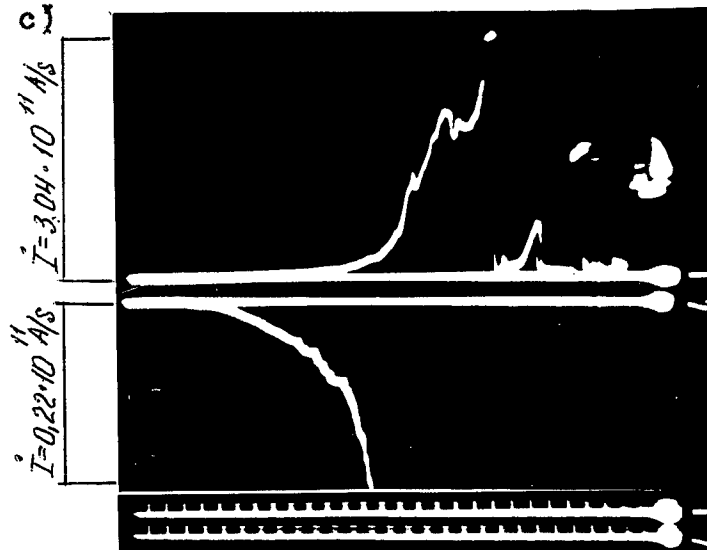


Fig. 3.14

Shot 3

EMG current dependence on time

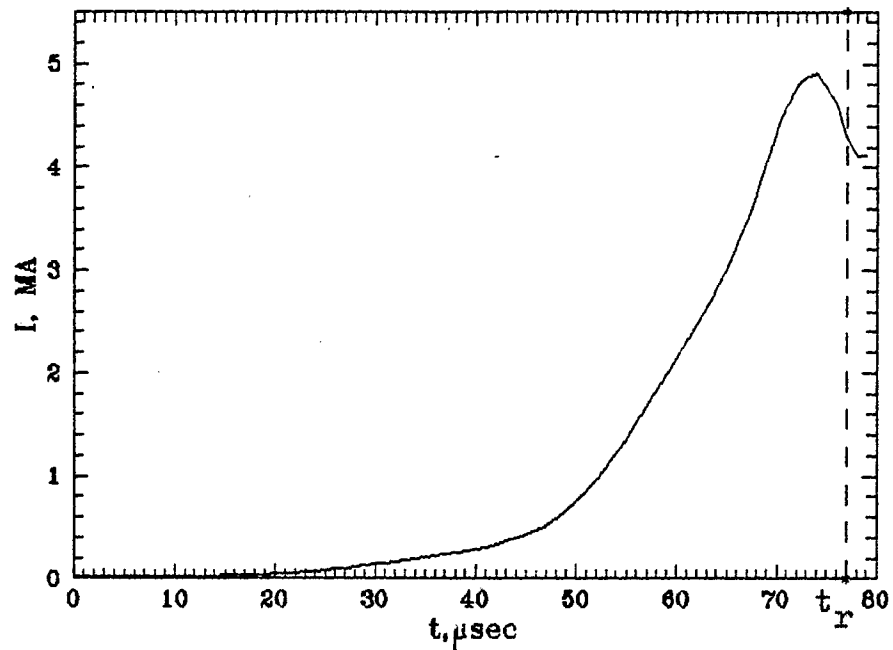


Fig.3.15

Liner radius dependence on time

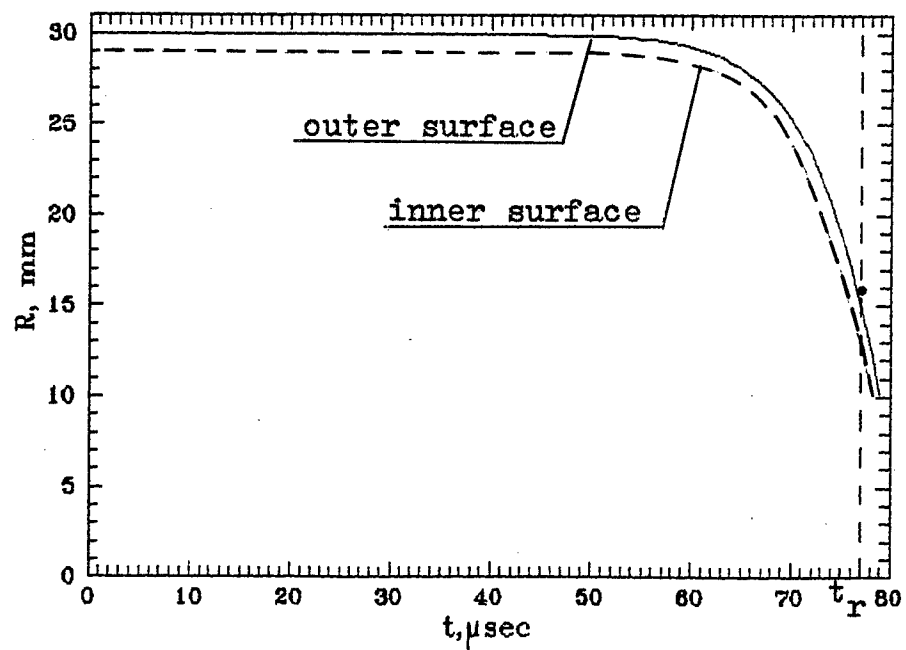


Fig.3.16



Fig. 3.14 (a,b,c) give oscillograms, obtained in the shot.

Fig. 3.15 shows the dependence of EMG current on time. Fig 3.16 shows the estimated dependences of liner radii on time. The point in the same picture shows the radius of an outer surface of the central liner part, obtained in the shot at the moment  $t_r$ .

The main experimental data are :  $t_r = 77 \mu\text{sec}$ ,  $I_{\text{max}} = 4,9 \text{ MA}$ ,  
 $I_r = 4,4 \text{ MA}$ ,  $Y_r = 2,8 \cdot 10^8 \text{ A}^2 \cdot \text{s}$ ,  $Z_r = 2,2 \cdot 10^3 \text{ A}^2 \cdot \text{s}^2$ ,  $R_r = 0,53 R_0 = 16 \text{ mm}$

#### SHOT 4

The goal of the shot was to define the picture of liner expansion after a moment of focusing.

Under focusing we understand the moment when the inner surface of a liner stops effected by counterpressure forces and its velocity becomes equal to zero.

Radii of focusing of inner and outer liner surfaces depend on many factors : density of liner material, magnetic pressure, state and properties of medium inside a liner, temperature of heating, etc.. After the moment of focusing the back process takes place : liner expands backwards.

For tests we chose a liner system, where to increase flight velocity the thickness of a left liner (located between conical electrodes with  $3^\circ$  angle) was the same as in the previous shots and was 1 mm (Fig. 3.17).

As it is seen from an x - ray picture (Fig. 3.18) a left liner accepted a shape of prolonged along a radius ellipsoid, the ends of a liner did not separate from electrode walls, but remained compressed along the radius. The ends of a liner, located between conical electrodes, partially exploded and separated from the walls. A radius of a central part of the liner is less than that of a left one, which is more thin.

Fig. 3.19 (a,b,c) shows oscillographs, obtained in the shot.

Fig. 3.20 shows dependence of EMG current on time.

Shot 4  
LS design

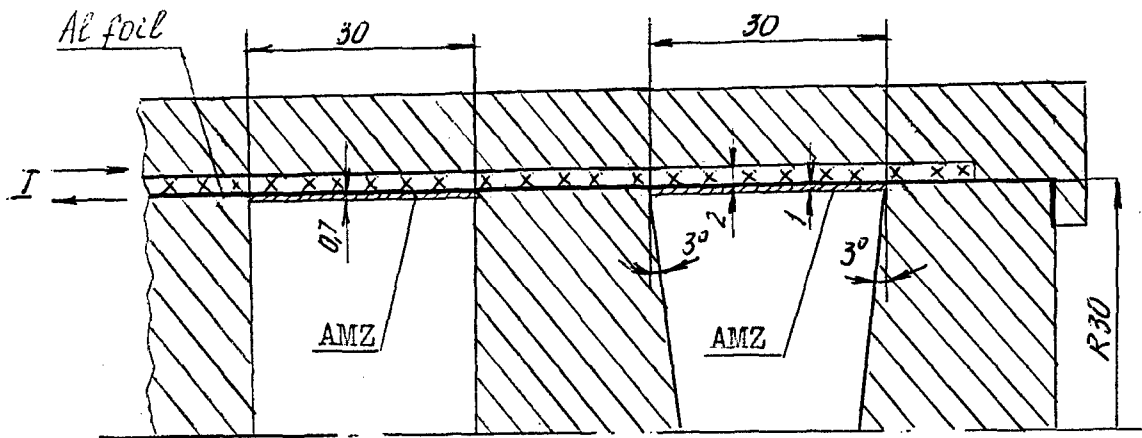


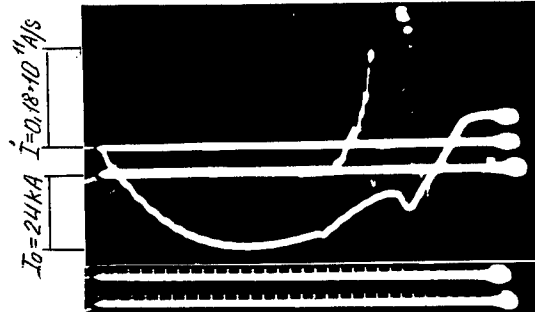
Fig. 3.17

Radiograph  
(working picture -  $t_r = 75 \mu\text{sec}$ )



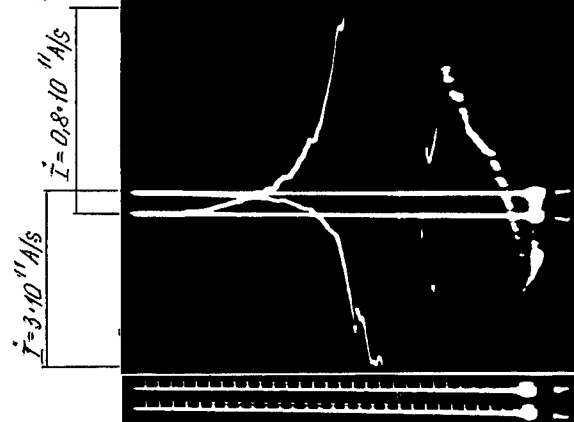
Fig. 3.18

a)



1 point = 4  $\mu\text{sec}$

b)



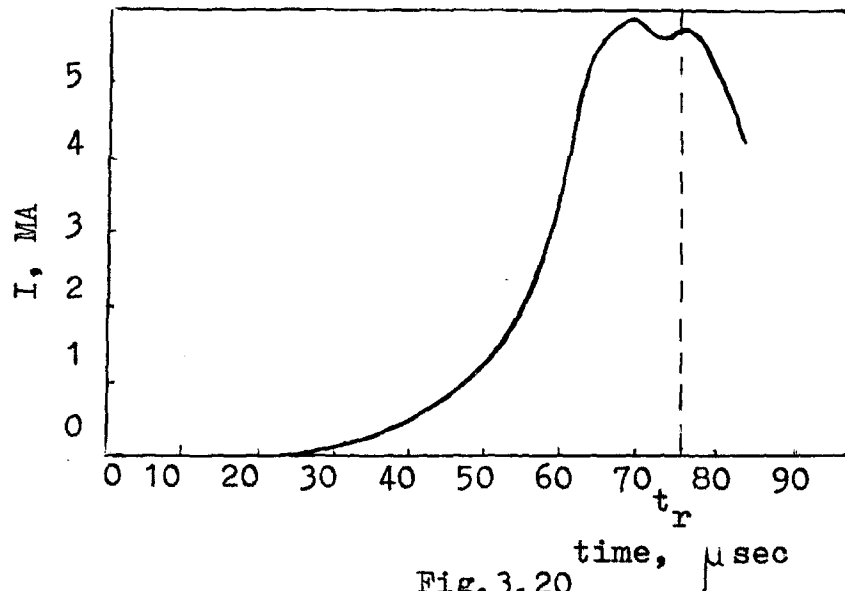
1 point = 4  $\mu\text{sec}$

c)

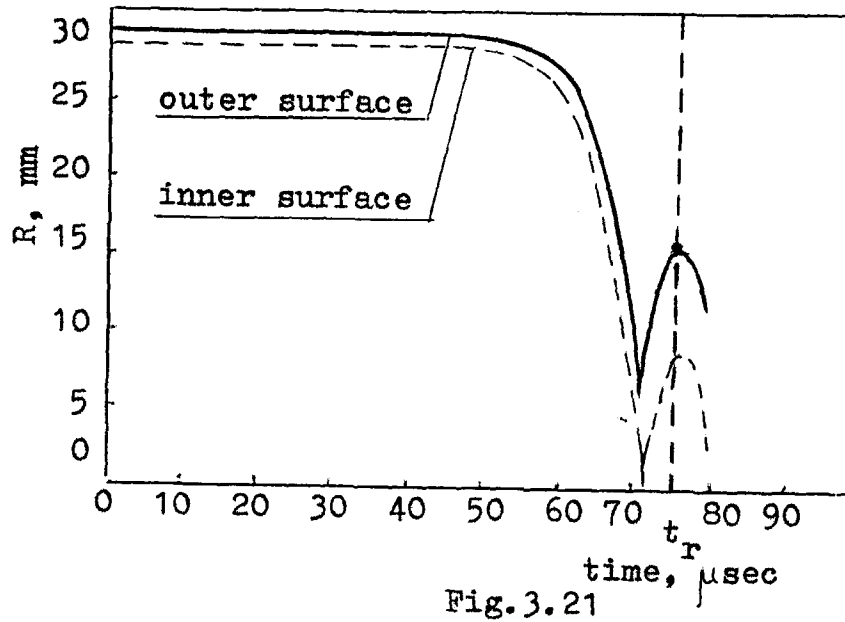


0.7 mm liner  
(0,7 mm thickness)

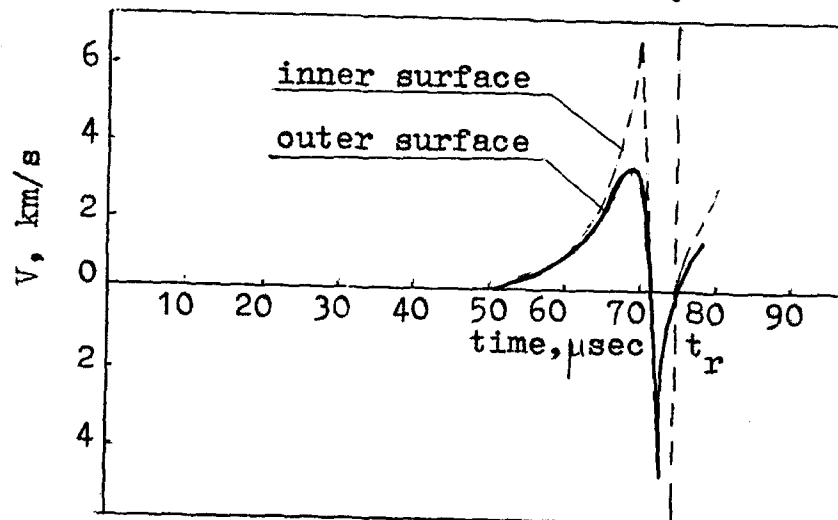
EMG current dependence on time



Dependence of a liner radius on time



Dependence of liner velocity on time



Shot 4  
The right liner  
(1 mm thickness)

Dependence of a liner radius on time

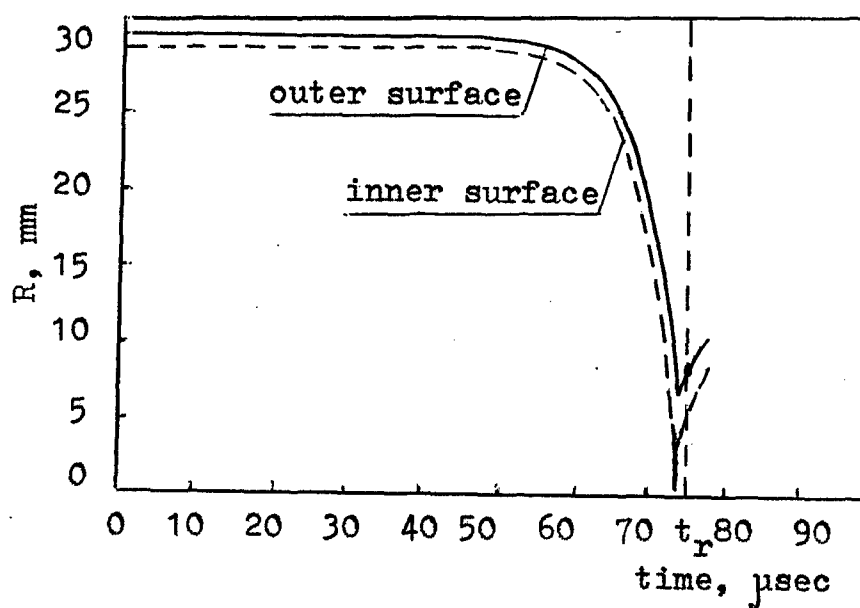


Fig. 3.23

Dependence of a liner velocity on time

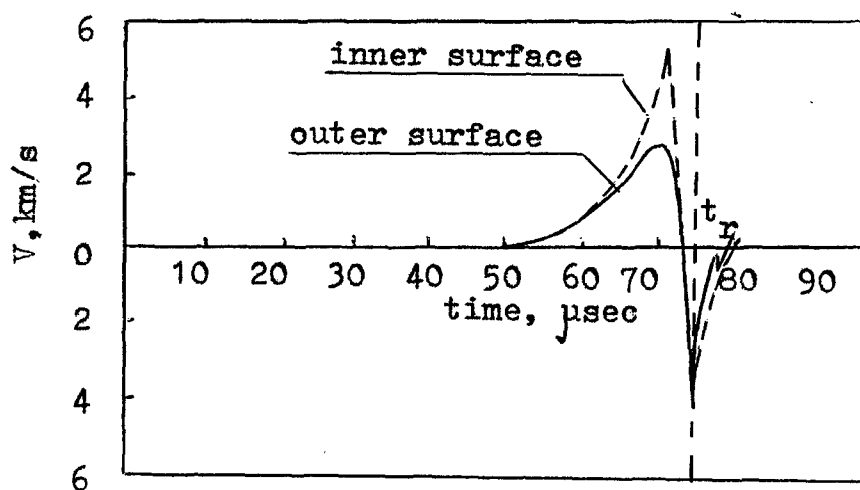


Fig. 3.24

As a result of the experiment it is obtained:

$t_r = 75 \mu\text{sec}$ ,  $I_{\text{max}} = 5,9 \text{ MA}$ ,  $I_r = 5,8 \text{ MA}$ ,  $Y_r = 4,7 \cdot 10^8 \text{ A}^2 \cdot \text{s}$ ,  $Z_r = 3,5 \cdot 10^3 \text{ A}^2 \cdot \text{s}^2$ .

1-D MHD calculations showed that the liners over the moment of radiography came through focusing and came up to the stage of expansion.

Calculation results of radii and velocities depending on time are given in Fig. 3.21, 3.22 for a left liner, in Fig. 3.23, 3.24 for a right liner.

According to estimations the focusing of a left liner 0,7 mm thick must take place at the moment of  $t_{1f} = 71 \mu\text{sec}$  (Fig. 3.21), focusing of a right, a thicker one, at the moment of  $t_{2f} = 73 \mu\text{sec}$  (Fig. 3.23).

In the experiment radiography was made at the moment of  $t_r = 75 \mu\text{sec}$ , i.e. after expansion.

By this moment the outer surface of a left liner has expanded along the radius from the axis by 16 mm (Fig. 3.21), the outer surface of a right liner - by 9 mm (Fig. 3.23).

This matches well with experimental data, which are shown by a point in these pictures. It goes out of calculations that to the moment of focusing the peak velocity of a left liner outer surface of 0,7 mm thick was 3,3 km/sec, that of an inner surface was 7,6 km/sec (Fig. 3.22). At the same time the velocity of a right liner of 1 mm thick was 2,8 km/sec and 5,4 km/sec, correspondingly (Fig. 3.24).

The analysis of results of the first set of experiments showed the unstable picture of interaction between liners and walls for the both methods of connection ("joint" and "over lapping").

The most probable reason of this instability is the presense of gaps between liner ends and electrodes.

This means that a special attention must be paid to the quality of connection between liners and electrode walls along the whole perimeter.

## THE SECOND SET OF EXPERIMENTS

In this set of experiments we tested the improved version of a liner system, where we took measures and provided more tight contact between liner ends and electrode walls. For this purpose overlapping liners were mounted on the electrode plateau 1,0 mm thick and were fixed there by a method of hot fit.

While designing liners and electrodes the tolerance for these elements has been chosen in such a way that a liner slipped over the plateau of electrodes only in a heated state. In the process of cooling up to the normal temperature a liner compressed and with its inner surface tightly came across the plateau surface of electrodes, providing in such a way a reliable electrical contact along the whole perimeter of a liner inner side.

To avoid local explosions on the surface of electrodes, the last were made out of steel (mark 30), liners themselves were made of aluminum (mark A 995).

### SHOT 5

A design of a liner system with a new method of joint is given in Fig. 3.25. LS radiograph at the moment  $t_r = 73 \mu\text{sec}$  is given in Fig. 3.26.

As it is seen from a radiograph, a constant contact between liner ends and electrode walls has been retained up to the moment of radiography using this method of fix. No local explosions on the surface of liners and walls were observed. At the moment of radiography liner edges were ahead of a central part which moved symmetrically.

In both portions (both with flat and conical electrodes with an angle of  $3^\circ$ ) the external liner radius  $R_r = 17$  mm and shape are practically equal.

Fig. 3.27 (a,b,c) shows oscillographs from the experiment, Fig. 3.28 shows current dependence on time.

Fig. 3.29 shows the dependence of a liner radius on time. The

Shot 5  
LS design

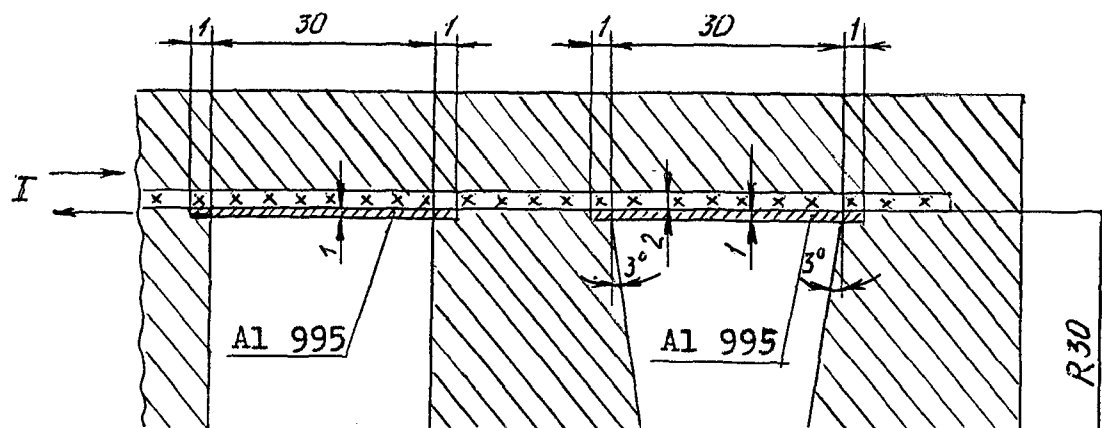


Fig. 3. 25.

## Radiograph

(working picture -  $t_r = 73 \mu\text{sec}$ )

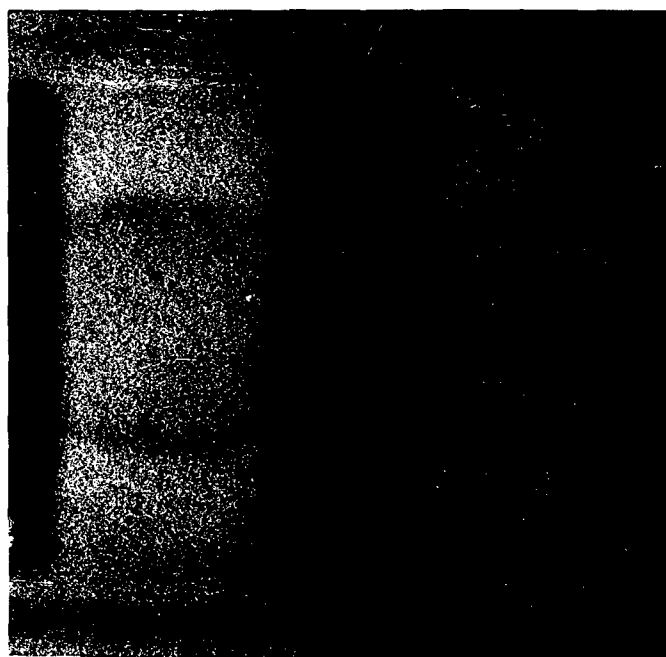
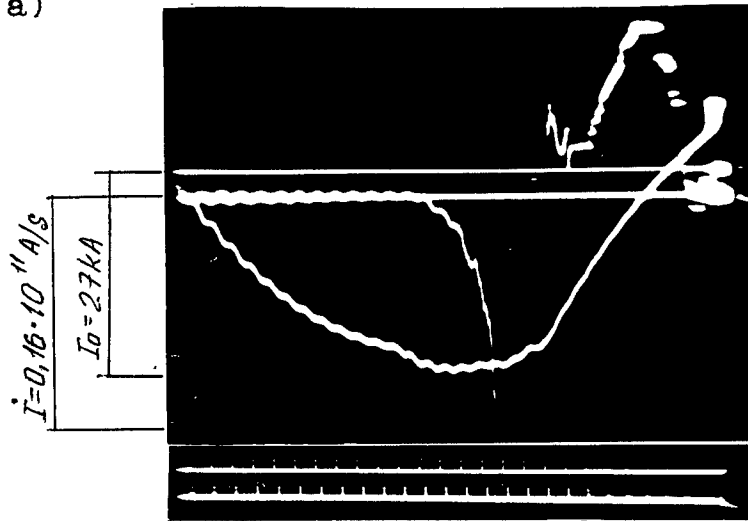


Fig. 3. 26



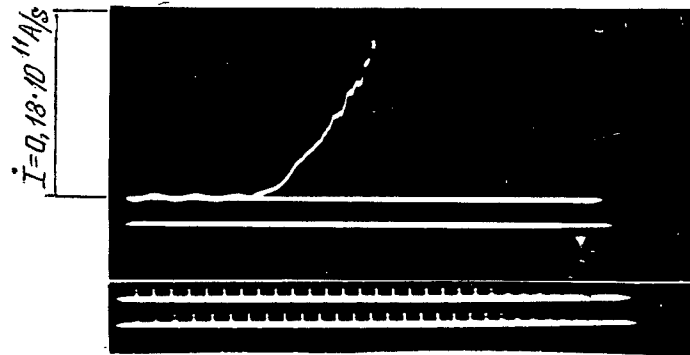
Shot 5  
Oscillograms  
1 point = 10  $\mu$ sec

a)



1 point = 4  $\mu$ sec

b)



1 point = 4  $\mu$ sec

c)

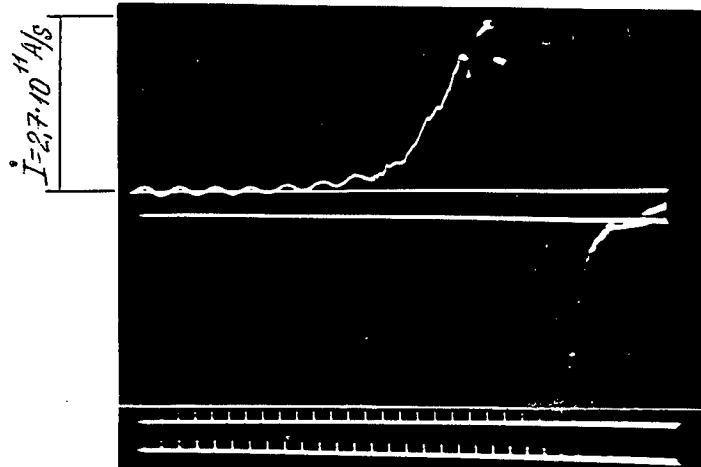


Fig. 3.27

EMG current dependence on time

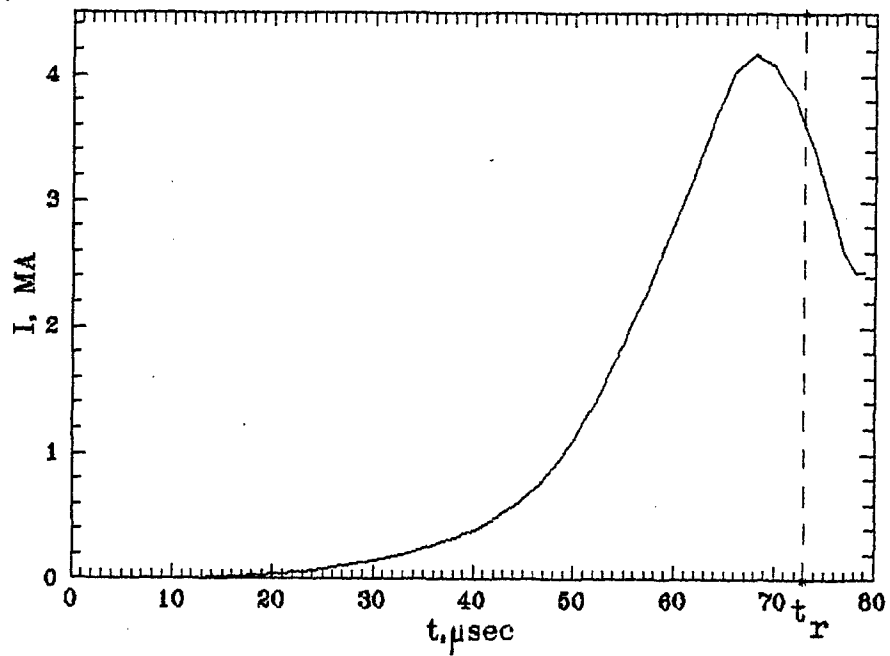


Fig. 3.28

Dependence of a liner radius on time

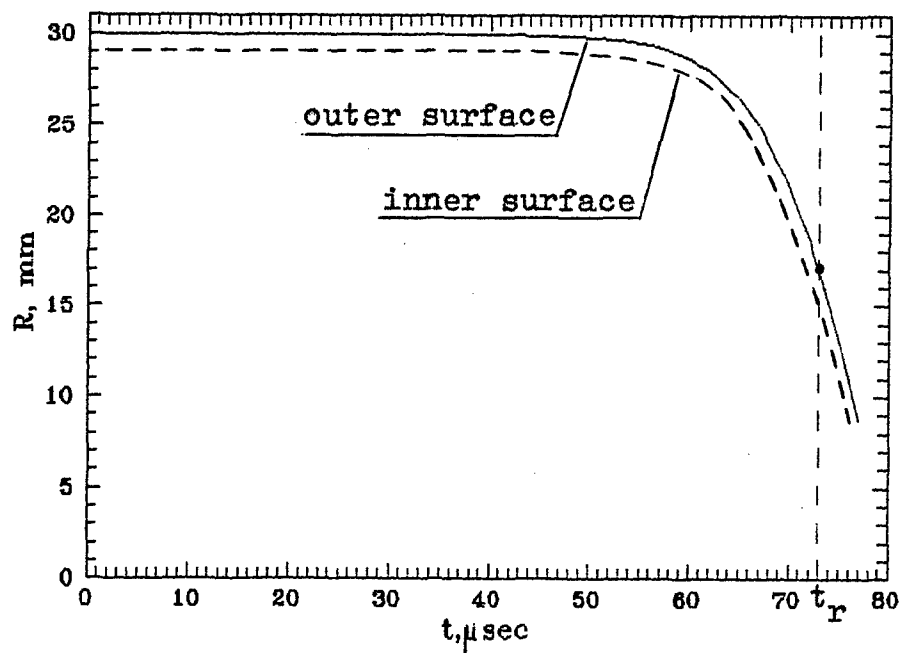


Fig. 3.29

point on the same dependence shows the external liner radius obtained in the experiment.

During the shot the following numbers were obtained:

$t_r = 73 \mu\text{sec}$ ,  $I_{\text{max}} = 4,18 \text{ MA}$ ,  $I_r = 3,61 \text{ MA}$ ,  $Y_r = 2,3 \cdot 10^8 \text{ A}^2 \cdot \text{s}$ ,  $Z_r = 1,93 \cdot 10^3 \text{ A}^2 \cdot \text{s}^2$ ,  
 $R_r = 0,57 \text{ Ro} = 17 \text{ mm}$ .

#### SHOT 6

To confirm the result obtained above, we conducted the second shot with the same LS. Unfortunately in this shot we managed to photograph only a liner between conical electrodes because of light marks on a part of an x - ray film.

A radiograph of the shot was shown in Fig. 3.31. It is seen from a radiograph that in this shot and in the shot 5 a contact between liner ends and the walls of conical electrode has been retained.

The oscillographs of the experiment are given in Fig. 3.32 (a,b,c).

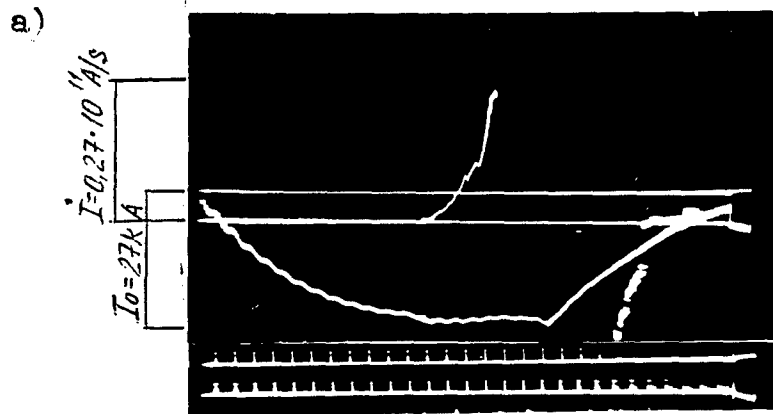
Fig. 3.33 shows EMG current dependence on time, Fig. 3.34 shows estimated radius dependence on time.

The following numbers are obtained in the shot.

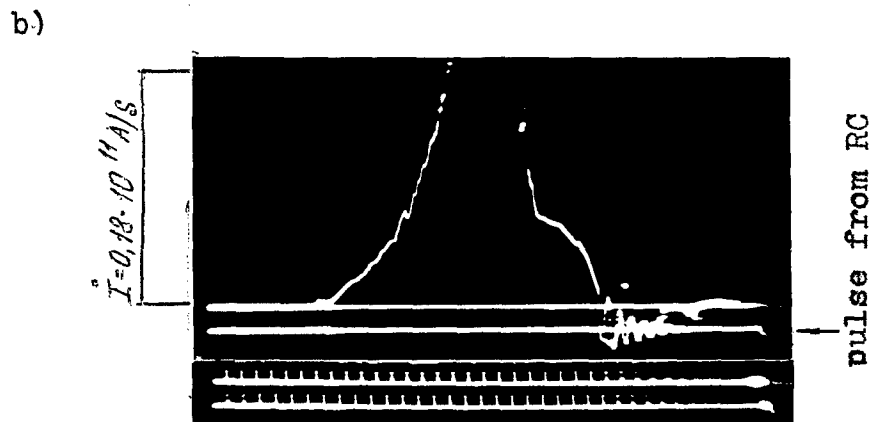
$t_r = 72,7 \mu\text{sec}$ ,  $I_{\text{max}} = 3,98 \text{ MA}$ ,  $I_r = 3,3 \text{ MA}$ ,  $Y_r = 2,1 \cdot 10^8 \text{ A}^2 \cdot \text{s}$ ,  $Z_r = 1,78 \cdot 10^3 \text{ A}^2 \cdot \text{s}^2$ ,  
 $R_r = 0,6 \text{ Ro} = 18 \text{ mm}$ .



Shot 6  
Oscillograms  
1 point = 10  $\mu$ sec



1 point = 4  $\mu$ sec



1 point = 4  $\mu$ sec

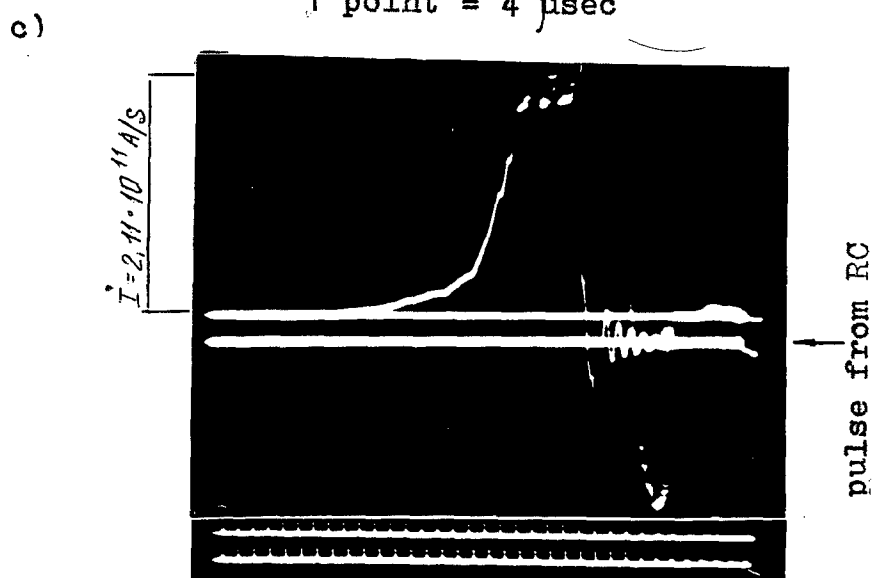


Fig. 3.32

## Shot 6

## EMG current dependence on time

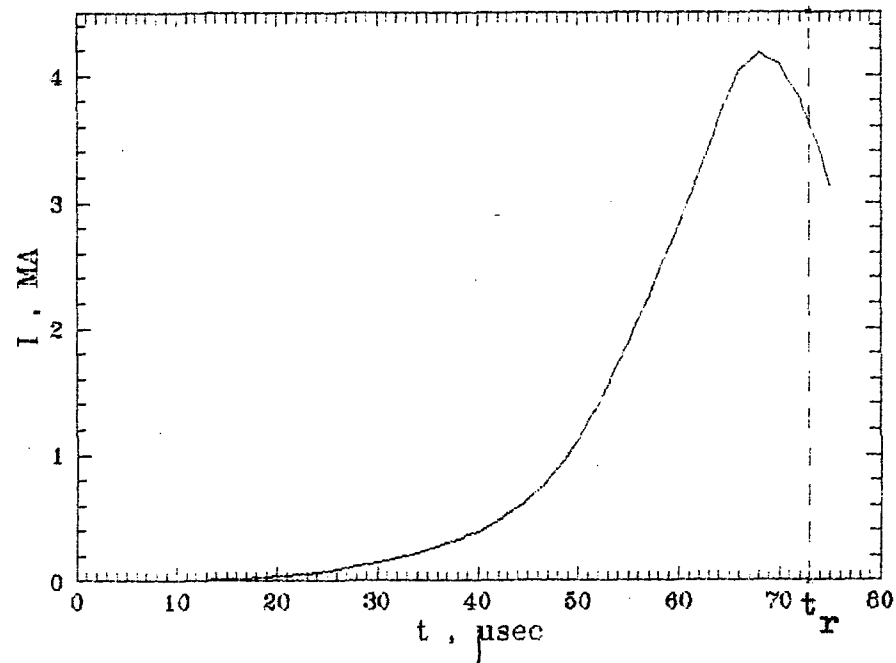


Fig. 3.33

## Dependence of liner radius on time

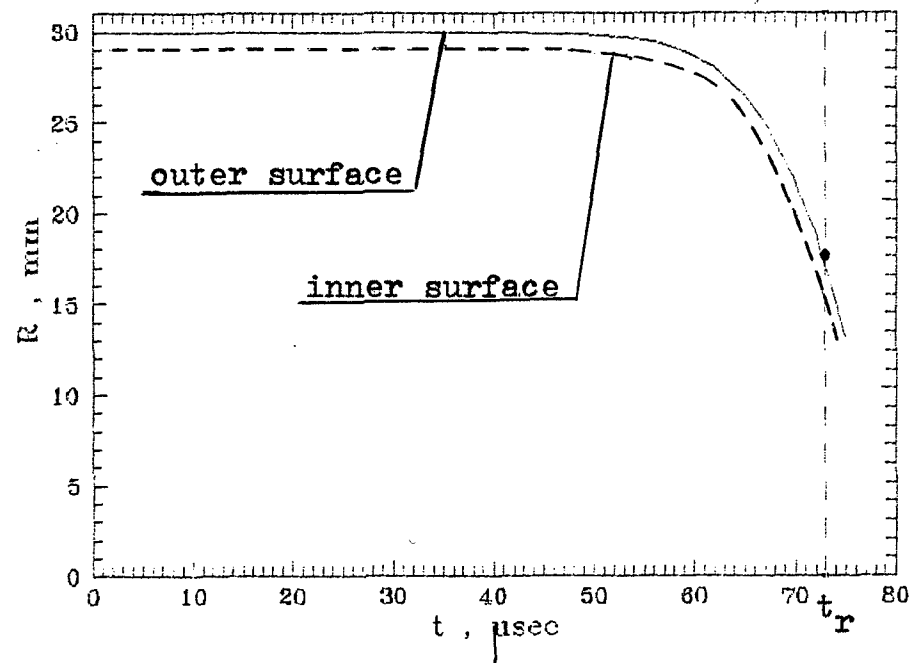


Fig. 3.34

#### 4. DISCUSSION OF EXPERIMENTAL RESULTS

The experiments with LS, conducted with various EMG currents, showed the significant effect of a method to fix a liner with electrode walls on the symmetry of a liner flight, especially in the wall area.

The first set of experiments was devoted to clarification of the fact : what is the reason for instability. Instability manifested itself in the fact that in experiments both with straight and conical electrodes, conducted in similar conditions, electrical explosion of liner ends and their separation from walls either took place or not. The only reason which could explain somehow the instability is that there are probably some joint gaps along the perimeter of a liner.

In the second set of experiments we used a known method of connection (hot fit of a line into electrode plateau), which enabled to exclude the separation of liner ends from the walls at the earliest stages of movement.

The x - ray data showed that with the chosen EMG modes axial convergence symmetry of central liner parts is satisfactory, despite the fact that the liners flew the distance, equal to 15 or 20 of their initial thickness.

It is important to notice that appearance of current azimuthal asymmetry in one of LS portions (e.g. Fig. 3.7 : a liner is to the left) does not lead to significant asymmetry in an adjacent portion (the same Fig. : a liner is to the right), though these liners were included in one and the same discharge circuit.

Taking into account magnetic field diffusion by MHD code we made a temperature estimation of a liner surface heat for shot 2, where LS radiography was made at the moment close to the moment of focusing. The calculation showed that the temperature of an outer surface did not exceed  $1250^{\circ}\text{C}$ , the temperature of an inner surface that of  $300^{\circ}\text{C}$ , i.e. an outer surface must be in a liquid state, an inner surface must be in a solid state.

To illustrate this for shot 2 we calculated the heat temperature and the metal density of a liner wall according to

its cross-section at the moment of radiography  $t_r=76,6 \mu\text{sec}$  and at the moment of focusing  $t_f=78.02 \mu\text{sec}$ .

As it is seen from Fig. 4.1 at the moment  $t_r$ , when the wall thickness reached the value of  $\Delta r=4,2 \text{ mm}$ , only 15% of its thickness (if to count from an external surface to an internal one) goes into a liquid state, the remaining part of a liner is in a solid state. In the moment of focusing ( $t_f$ ), when  $\Delta f=6 \text{ mm}$ , most part of the metal goes into a liquid state, excluding a medium layer. At this moment the peak density of compressed metal in the layers close to the inner liner surface was  $\rho_f=4,8 \text{ g/cm}^3$ .

As it is known from work [7], while accelerating flat metallic plates by the magnetic field the plate velocity is proportional to the value of current effect integral, the flight distance is proportional to the double integral of current effect.

If we admit a double integral as a criterion for cylindrical liners, which defines the radius of liner compression provided that commutation effect, when cylindrical liners converge to the center up to  $R=0,3 R_0$ , is not large, let us imagine the set of experiments as the dependence  $R=f(Z)$ , where  $R$  is a liner radius,  $Z$  is a double integral of current effect.

The estimated dependence for an aluminum liner with a 30 mm radius and 1 mm thickness wall is shown in Fig. 4.2. As it is seen from the plot, estimated dependence looks like a linear one. The points in the plot denote radii, obtained in the experiments. The arrow in the axis of abscissa shows the double integral, with which the focusing of a liner system takes place.

It goes from the plot that a liner focusing with 30 mm radius and 1 mm thickness wall takes place with double integral not less than  $Z_f = 3,3 \cdot 10^3 \text{ A}^2 \cdot \text{s}^2$ .



Estimated dependences of temperature and liner material density according to thickness at the moments of radiography and focusing

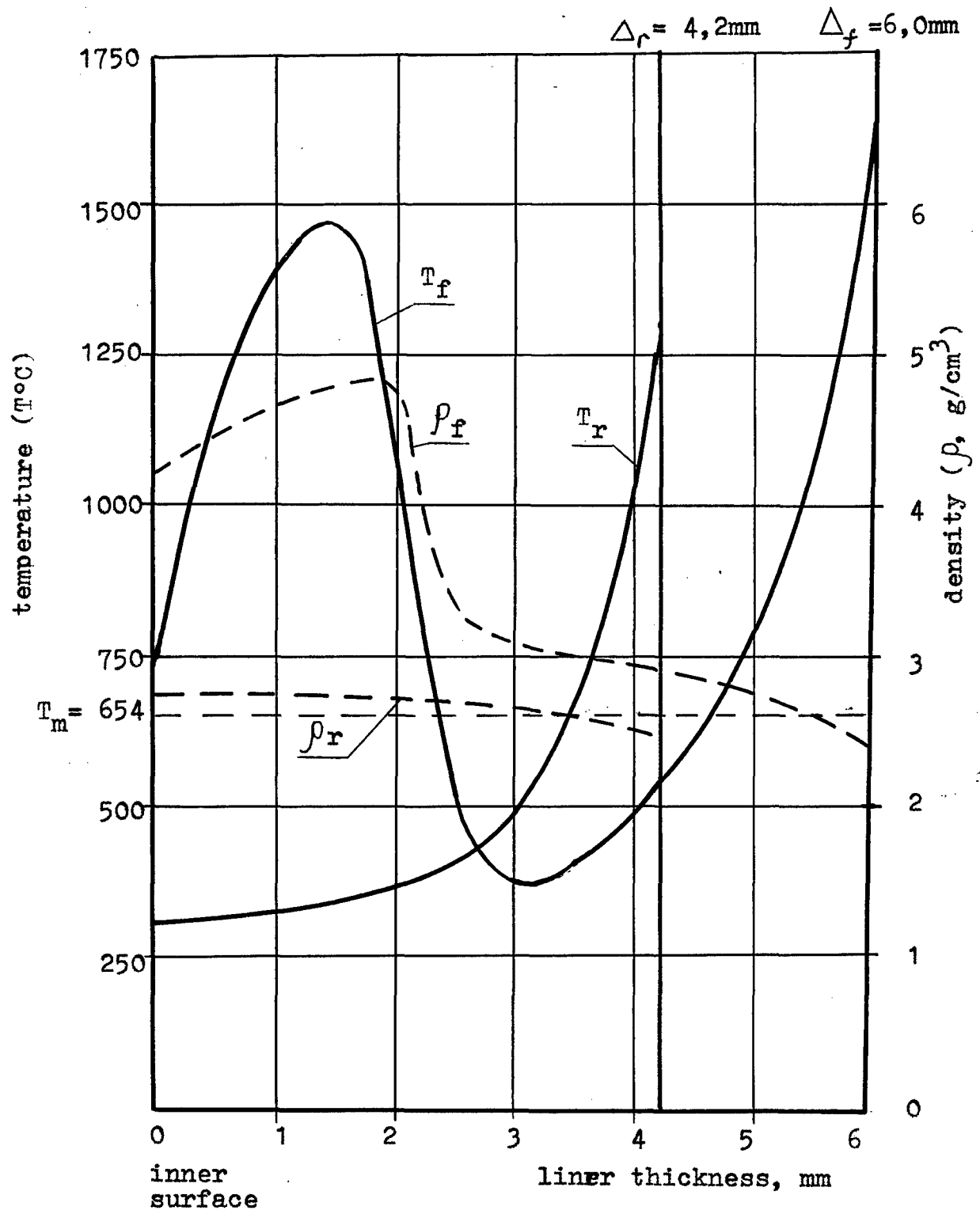
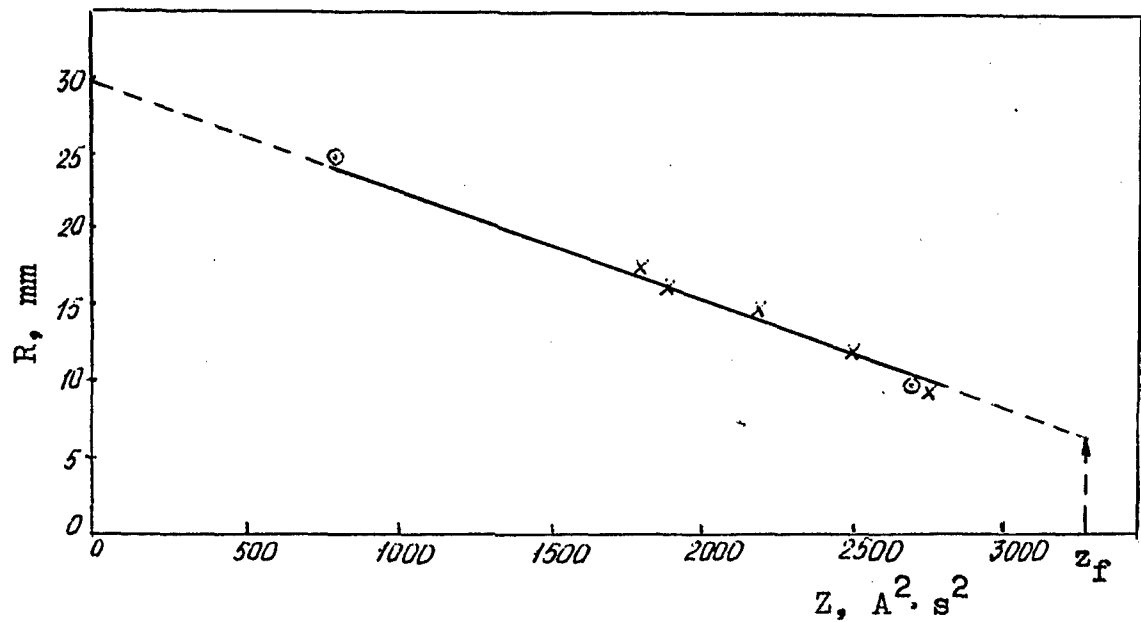


Fig. 4.1

Dependence of a liner radius on double  
integral of current effect



Experimental data taken from the report /4/  
are designated by the sig  $\odot$

Fig. 4.2

Two sets of explosive experiments with double liner systems have been conducted. A helical generator of 100 mm diameter and 700 mm length was used as a source of energy. The source provided 5,9 MA amplitude current pulses in a liner system.

The first set of experiments was carried out aiming to study wall effects and to choose the method how to joint a liner with electrodes with which the continues contact of a liner with electrode walls would be provided. As a joint method we chose the method of "hot fit". The joint enabled to provide the tight and reliable electric contact of a liner with electrode walls.

In a two-liner system the axial asymmetry in one of liners does not lead to a simmlar asymmetry in another one, though both liners are included in one discharge circiut of a generator and one and the same current flew through them.

With discharge currents up to 5,9 MA the axial symmetry of convergence of liner central parts visually is quite satisfactory, despite the fact that liners have flown distances, equal to 15-20 inherent inital thickness.

Flight velocities of liners were calculated by 1-D MHD code. The calculation showed that the velocity of a central part external boundary of an aluminum liner with 30 mm radius, initial wall thickness of 1 mm with a maximum discharge current of 5,8 Ma was  $\sim 2,8$  km/sec at the moment of focusing; the velocity of an inner surface was 5,4 km/sec. For the liners with 0,7 mm wall thickness the numbers were  $\sim 3,3$  km/sec, 7,6 km/sec, correspondingly.

According to the results of one of calculations we built the dependence of temperature distribution according to a liner wall cross - section at the moment of radiography and the moments of focusing. According to the calculation the heat temperature of liner walls did not exceed the temperature of evaporation of aluminum.

We compared the estimated dependence of liner compression radius on double integral of current effect with the experimental results. The matching of data is satisfactory.

1. Pavlovskii A. I. Ultrahigh Magnetic Fields Cumulation. Megagauss Fields and Pulsed Power Systems. MG-V, Edited by V. M. Titov and G. A. Shvetsov. Nova Science Publishers, New York, p. 1-13.
2. Degnan J. H., Baker W. L., Beason J. D., Clouse C. J., Dietz D., Hall D. J., Holmes J. L., Price D. W., Sovinio C. R. et al. Multi-Megajoule Shaped Solid Liner Implosions: Ibid, p. 623-630.
3. Degnan J. H., Alme M. L., Baker W. L., Buff J. S. et al. Multi-megajoule Solid Liner Implosions. Megagauss Technology and Pulsed Power Applications. MG-IV, Edited by C. M. Fowler, R. S. Caird and D. J. Erickson. Plenum Press, New York and London, 1987, p. 699-706.
4. Chernyshev V. K., Zharinov Ye. I., Kudelkin I. D., Buzin V. N., Ionov A. I., Grinevich B. Ye., Vlasova M. A., Yegorychev B. T., Yerichev V. N. et al. Cylindrical Liner: Implosion Dynamics Under EMG Magnetic Pressure. Book of Abstracts. MG-VI, 1992, Albuquerque, New Mexico (USA), p. 92.
5. Кудрявцев И. Б., Лужников Л. П. Материалы в машиностроении (ч. 1), Москва, Машиностроение, 1967, с. 20.
6. Bujko A. M., Garanin S. F., Demidov V. A., Kostjukov V. N., Kuzjaev A. I., Kulagin A. A., Mamyshev V. I., Mokhov V. N., Petrukhin A. A., Piskarev P. N., Protasov M. S., Chernyshev V. K., Yakubov V. B. Investigation of Dynamics of a Cylindrical Exploding Liner Accelerated by a Magnetic Field in the Megagauss Field Range. Megagauss Fields and Pulsed Power Systems. Edit. by V. M. Titov and G. A. Shvetsov. VG-V, Nova Science Publishers, p. 743.
7. Чернышев В. К., Жаринов Е. И., Гриневич Б. Е., Куделькин И. Д., Бузин В. Н., Зимаков С. Д., Ионов А. И., Егорычев Б. Т., Еричев В. Н. Ускорение плоских металлических и диэлектрических лайнеров магнитным полем. Забобахинские научные чтения 14-17 января 1992 г. (тезисы докладов), Быштым, Дальняя Дача.